frontiers | Frontiers in Plant Science

TYPE Original Research
PUBLISHED 12 April 2024
DOI 10.3389/fpls.2024.1369299

Check for updates

OPEN ACCESS

EDITED BY
Mingyue Gou,
Henan Agricultural University, China

REVIEWED BY
Deepak Singla,
Punjab Agricultural University, India
Wei-Hua Tang,
Chinese Academy of Sciences (CAS), China

*CORRESPONDENCE
Guus Bakkeren
guus.bakkeren@agr.gc.ca

RECEIVED 12 January 2024
ACCEPTED 19 February 2024
PUBLISHED 12 April 2024

CITATION
Sun S and Bakkeren G (2024) A bird's-eye view: exploration of the flavin-containing monooxygenase superfamily in common wheat.
Front. Plant Sci. 15:1369299.
doi: 10.3389/fpls.2024.1369299

COPYRIGHT
© 2024 Sherry Sun and His Majesty the King in Right of Canada, as represented by the Minister of Agriculture and Agri-Food Canada for the contribution of Guus Bakkeren. This is an open-access article distributed under the terms of the Creative Commons Attribution License (CC BY). The use, distribution or reproduction in other forums is permitted, provided the original author(s) and the copyright owner(s) are credited and that the original publication in this journal is cited, in accordance with accepted academic practice. No use, distribution or reproduction is permitted which does not comply with these terms.

A bird's-eye view: exploration of the flavin-containing monooxygenase superfamily in common wheat

Sherry Sun [1] and Guus Bakkeren [2*]

[1]Department of Botany, The University of British Columbia, Vancouver, BC, Canada, [2]Agriculture and Agri-Food Canada, Summerland Research & Development Center, Summerland, BC, Canada

The Flavin Monooxygenase (*FMO*) gene superfamily in plants is involved in various processes most widely documented for its involvement in auxin biosynthesis, specialized metabolite biosynthesis, and plant microbial defense signaling. The roles of FMOs in defense signaling and disease resistance have recently come into focus as they may present opportunities to increase immune responses in plants including leading to systemic acquired resistance, but are not well characterized. We present a comprehensive catalogue of *FMO*s found in genomes across vascular plants and explore, in depth, 170 wheat *TaFMO* genes for sequence architecture, *cis*-acting regulatory elements, and changes due to Transposable Element insertions. A molecular phylogeny separates TaFMOs into three clades (A, B, and C) for which we further report gene duplication patterns, and differential rates of homoeologue expansion and retention among TaFMO subclades. We discuss Clade B TaFMOs where gene expansion is similarly seen in other cereal genomes. Transcriptome data from various studies point towards involvement of subclade B2 *TaFMO*s in disease responses against both biotrophic and necrotrophic pathogens, substantiated by promoter element analysis. We hypothesize that certain TaFMOs are responsive to both abiotic and biotic stresses, providing potential targets for enhancing disease resistance, plant yield and other important agronomic traits. Altogether, FMOs in wheat and other crop plants present an untapped resource to be exploited for improving the quality of crops.

KEYWORDS

disease resistance, FMO, gene family, phylogenetics, wheat

1 Introduction

Flavin-containing monooxygenases (FMOs; EC 1.14.13.8) constitute a ubiquitous class of ancient, highly-conserved enzymes that have been well-characterized in bacteria, fungi, and insects, catalyzing the transformations of many molecules across all domains of life (Eswaramoorthy et al., 2006; Huijbers et al., 2014; Mascotti et al., 2015). FMOs are dimeric in nature, with Rossman folds in a bi-lateral distribution containing FAD- and NAD(P)H-

binding domains (Schlaich, 2007; Rossner et al., 2017; Thodberg and Jakobsen Neilson, 2020). Typically, FMOs act on small, nucleophilic substrates that contain either a sulfur (S) or nitrogen (N) atom, resulting in the oxygenation of a wide range of compounds; this process often aides in the detoxification of xenobiotic compounds in many organisms (Eswaramoorthy et al., 2006). While FMOs are well characterized in bacteria, fungi, and insects, less is known of many of the FMOs in vascular plants, despite abundant putative plant FMOs having been observed (Schlaich, 2007).

Multiple studies from the last two decades indicate that a distinct subset of plant FMOs have evolved to participate in biosynthesis of auxin, a crucial hormone for plant growth (Kendrew, 2001; Schlaich, 2007; Yamamoto et al., 2007; Zhao, 2014). This specialized group of plant FMOs has been coined 'YUCCA', named after the phenotype of a dominant *Arabidopsis thaliana fmo* deletion mutant resembling the yucca plant (Zhao et al., 2001) and many of which have been functionally characterized in this model plant (Cao et al., 2019; Qin et al., 2020). Due to the significance auxin biosynthesis has on plant growth, development, and yield in crop plants, many studies since then have focused on identifying and characterizing the orthologous 'YUCCA' FMOs across a range of commercially valuable plant species, such as apple, peach, soybean, and rice (Yamamoto et al., 2007; Qin et al., 2020; Song et al., 2020; Luo et al., 2022; Zhang et al., 2022). Additionally, a subset of FMOs in *A. thaliana* have been characterized for their activity in the *S*-oxygenation of sidechains in various glucosinolate (GSL) compounds (Li et al., 2011). GSLs are potent, specialized defense metabolites found exclusively in the order Brassicales known to play a major role against insect herbivory (Kong et al., 2016; Cang et al., 2018). Grouped as "FMO-GSOXs", these FMOs, which participate in processing metabolites, play a significant defensive role in plants that produce GSLs. Of the 29 total identified FMOs in *A. thaliana*, eleven are annotated to be YUCCAs, twelve are purportedly FMO-GS-OXs, one has been reported to be crucial for systemic acquired resistance (SAR) against microbial pathogens (Hartmann et al., 2018; Czarnocka et al., 2020), and five do not presently have designated functions. A recent review (Mitchell and Weng, 2019) provided a brief synopsis of these three groups of plant FMOs. Together these studies reveal that FMOs play diverse biological responses in plants, much of which have yet to be characterized.

Outside *A. thaliana*, much less is known about non-YUCCA FMOs, particularly in cereal crops such as *Triticum aestivum* (common bread wheat), an essential food source for over 50% of the world's population (Curtis and Halford, 2014). *Yang et al.* (Yang et al., 2021) focused on 'YUCCA' genes in wheat and identified 63 *TaYUCCA FMO* genes which they assigned to six subclades in a gene genealogy comparison; for a subset of these genes, they analyzed transcriptional activity using public transcriptomic data in an attempt to reveal function. Gaba et al. (2023) recently surveyed the genomes of ten different wild and cultivated rice species for *FMO* genes and revealed how little is presently known about FMOs outside the YUCCA group. Their study emphasized the need for more in-depth studies of other FMOs in crop plants.

Here, we address the extent to which *FMOs* have expanded across vascular plants by surveying comprehensively *FMO*-encoding genes across a broad range of plant taxa. We identified 170 likely wheat *FMOs* (*TaFMOs*) in the cultivar 'Chinese Spring' (the fully-sequenced reference genome, RefSeq v2.1), and sought to expand knowledge of the evolution, distribution, gene expansions, and potential functional diversity for different groups of *TaFMO* genes by using thorough phylogenetic, gene genealogy and transcriptome analyses using data obtained from publicly available studies. In addition, we take into account existing literature pertaining to *TaYUCCAs* (Li et al., 2014; Yang et al., 2021) and present a more cohesive picture of the biological roles that *TaFMOs* may play across a broad range of conditions, with a particular focus on various pathogen defense responses.

2 Materials and methods

2.1 Genome-wide identification of FMO genes

We obtained a protein-family hidden Markov model (HMM) profile for the FMO-like family (PF00743 v22) from the Protein Family (Pfam) database (https://pfam.xfam.org/), and conducted a local HMM search (HMMER v3.3.2; http://hmmer.org/) with significance parameters of *E*-value < $1e^{-2}$ against the International Wheat Genome Sequencing Consortium (IWGSC) fully-sequenced reference genomes for version RefSeqv2.1, to identify all putative wheat *flavin-containing monooxygenase* genes (*TaFMOs*) for the cultivar 'Chinese Spring'. Results from HMMER were further consolidated with the use of query-based searches in both the online database Wheat Proteome (Duncan et al., 2017) with the search term 'flavin-containing monooxygenase' and the search term 'flavin monooxygenase' in the UniProt database (https://www.uniprot.org/). Similarly, all *FMO* candidate genes from other plant species spanning a vast range of green plants and algae, were found through a HMM-based search. Table 1 lists the total number of FMOs per plant species. We used the summary of relationships of major angiosperm lineages available at NCBI Common Tree builder (https://www.ncbi.nlm.nih.gov/Taxonomy/CommonTree/wwwcmt.cgi) to display the distribution of FMOs in vascular plants (Figure 1; for sources of sequence and protein data and gene search details, see Supplementary Tables S1, S2; Appendix S1, Supplementary Figure S1).

TABLE 1 List of plant species in FMO search (HMM profile PF00743) and number of total FMOs found.

Species	Common Name	FMO total number
Aegilops tauschii	Goatgrass	62
Amborella trichopoda	Not Available	16
Arabidopsis lyrata	Lyre-leaved Rock Cress	23
Arabidopsis thaliana	Thale Cress	29
Beta vulgaris	Beet	14
Brachypodium distachyon	Stiff Brome	30
Brassica napus	Rapeseed	73

(Continued)

TABLE 1 Continued

Species	Common Name	FMO total number
Brassica oleracea	Cabbage/Broccolli/etc.	38
Corchorus capsularis	White Jute	26
Cucumis sativus	Cucumber	24
Galdieria sulphuraria	Red Microalga	1
Glycine max	Soybean	39
Gossypium raimondii	Cotton	27
Helianthus annuus	Sunflower	64
Hordeum vulgare	Barley	59
Leersia perrieri	Cutgrass	28
Lupinus angustifolius	Blue Lupin	24
Manihot esculenta	Cassava	26
Medicago truncatula	Alfalfa	29
Musa acuminata	Banana	33
Oryza sativa (sp. Japonica)	Rice	31
Panicum hallii	Panicgrass	28
Phaseolus vulgaris	Green Bean	18
Physcomitrium patens	Club Moss	14
Picea abies	Norway spruce	14
Populus trichocarpa	Poplar	25
Prunus persica	Peach	15
Selaginella moellendorffii	Spike Moss	16
Setaria italica	Foxtail millet	35
Solanum lycopersicum	Tomato	18
Solanum tuberosum	Potato	23
Sorghum bicolor	Sorghum	30
Theobroma cacao	Cocoa	16
Trifolium pratense	Red Clover	27
Triticum aestivum	Common Wheat	170
Triticum dicoccoides	Emmer Wheat	84
Triticum urartu	Einkorn Wheat	41
Vitis vinifera	Grape	33
Zea mays	Corn	37

2.2 Characterization of the TaFMO family genes

The full wheat cDNA, CDS, and peptide sequences of candidate *TaFMO* genes identified were retrieved from IWGSC (The International Wheat Genome Sequencing Consortium (IWGSC) et al., 2018). Gene Ontology (GO) terms were retrieved from the Uniprot database (https://www.uniprot.org/; accessed January 2023). The structure of exons and introns were determined using the CDS and gene sequences of *TaFMO*s analyzed with the Gene Structure Display Server (GSDS) version 2.0 (gsds.cbi.pku.edu.cn; Hu et al., 2015). A small subset of putative *TaFMOs* were represented by splice variants and included for downstream analyses, on the basis that each variant could encode for fully functioning TaFMO proteins acting in different tissues, conditions, and developmental stages.

To assess whether the enzymatic activity of each candidate TaFMO could be carried out, the presence of three previously well-described FMO motifs (Eswaramoorthy et al., 2006; Mishina and Zeier, 2006; Schlaich, 2007; Thodberg and Jakobsen Neilson, 2020) known to be crucial for cofactor binding and required for proper FMO function—the FAD- and NAD(P)H-binding motifs crucial for oxygenation activity, the FMO-identifying motif facilitating in NAD(P)H-binding at the core pocket of the enzyme, and the ATG-containing motif thought to govern hydroxylation activity—were assessed with multiple sequence alignments (MSA) using MAFFT with the E-INS-I setting; see Appendix S2 (Katoh et al., 2019). Candidates that did not possess one or all motifs were retained in downstream phylogenetic analyses but flagged as 'non-canonical' (nc) FMOs with the assumption that oxygenation activity may be compromised, as we used conservation of all motifs as a proxy for predicting FMO function. We predicted the putative protein structure of all TaFMOs using the Protein Homology/Analogy Recognition Engine V 2.0 (Phyre^2; Kelley et al., 2015) and then visualized them with PyMOL (Version 2.0 Schrödinger and DeLano, 2020). We used the Simple Modular Architecture Research Tool (SMART; https://smart.embl.de/; Letunic et al., 2021) program to gather protein domains for display (Figure 2). Possible transmembrane domains and signal peptides for all TaFMO were predicted using the programs DeepTMHMM and SignalP - 6.0 (Hallgren et al., 2022; Teufel et al., 2022).

2.3 Phylogenetic analyses of the TaFMO gene family and sub-families

We inferred a maximum likelihood (ML) phylogeny to define relationships between total validated *TaFMOs* and validated *FMO*s from the model plant *A. thaliana*, the cereal crop *Oryza sativa* subsp. *japonica*, and sister group of all other angiosperms, *Amborella trichopoda*. We selected a red algae having a single *FMO* as an outgroup. We first aligned full-length FMO peptide sequences using MAFFT with the E-INS-i setting (Katoh et al., 2019). We validated the full-length alignment of the total FMOs across plant species using the software HOMO v2.0 (Jermiin, 2017) by using it to determine whether all FMO sequences met the phylogenetic assumption of evolution under reversible, stationary, and globally homogenous conditions (Jermiin, 2017; Jermiin et al., 2020). Following this, poorly aligned regions of the MSA were masked using the AliStat program (Wong et al., 2014) to ensure downstream analysis focused on regions where

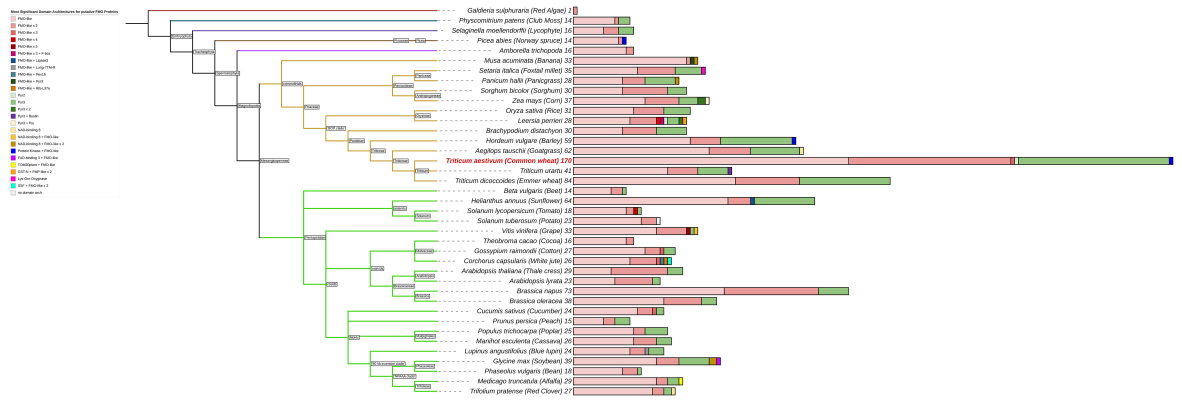

FIGURE 1
Total number of predicted FMOs and their main domain architectures as reported from Hidden Markov Modelling (HMM). Branch colors indicate major subdivisions amongst vascular plants. Total numbers of FMOs are reported as a number at the tips of each bar, and multivariate bars shows colors corresponding to the proportion of FMOs for each of the various kinds of domain architectures seen in the legend.

amino acid residues were readily alignable across sequences (see Appendix S2) (Wong et al., 2014). We then manually inspected alignments using Mesquite v 3.7 (Maddison and Maddison, 2023) and adjusted accordingly. Lastly, we used IQ-TREE v 2.2.0 to infer the ML tree based on amino acid alignments; we inferred the optimal substitution model using ModelFinder (JTT+I+G4), considering the Bayesian Information Criterion, BIC (Kalyaanamoorthy et al., 2017), and calculated branch support from 1000 standard bootstrapping

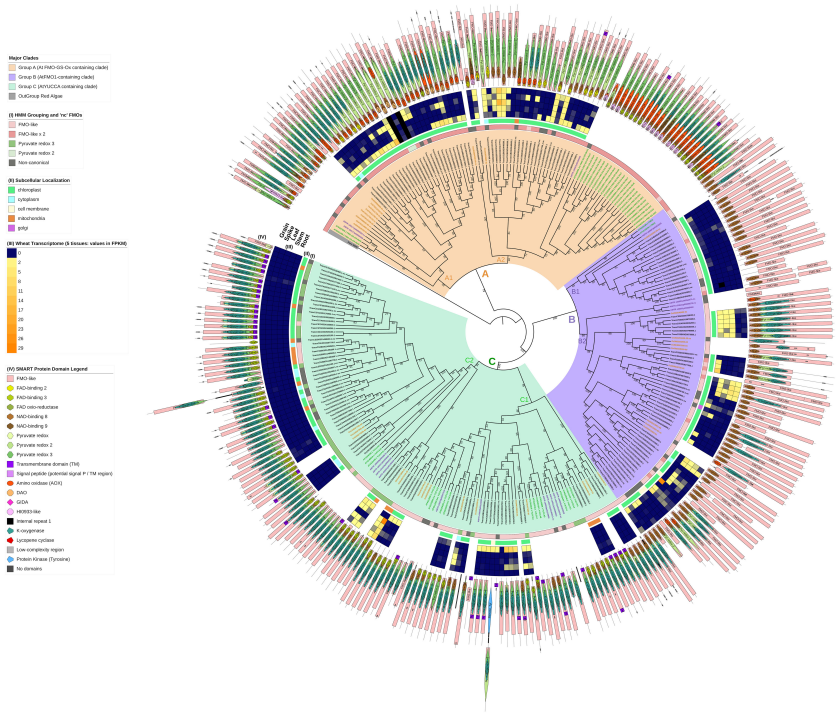

FIGURE 2
A maximum-likelihood (ML) consensus genealogy tree of total protein sequences of candidate TaFMOs (black gene IDs), OsjFMOs (yellow), AtFMOs (green), AmtriFMOs (purple), and GasuFMOs (grey). One GasuFMO (red microalgae) was used as outgroup. ML geneology was constructed from IQ-TREE (1000 standard bootstrap replicates, JTT+I+G4 substitution model). Three major subclades A (orange shading), B (purple) and C (green) were confidently supported across vascular plant FMOs. Outer circles: (I) shows the domain architecture the candidate FMO belongs to (from HMMER), as annotated in Figure 1; non-canonical 'nc' and truncated FMO protein candidates are marked with a dark grey box. (II) indicates predicted subcellular localization of TaFMO proteins. (III) represent transcript values (in FPKM) of each *TaFMO* candidate gene expressed under 5 tissue types (root, stem, leaves, spike, grain) from RNAseq experiments compiled on the Wheat Proteome database (Duncan et al., 2017). (IV) indicates SMART-predicted protein domains inclusive in each candidate FMO. Group A contains the least number of *TaFMOs*, totaling 55 splice variants pertaining to 39 genes (see S1 notes for explanation of exclusion of one *TaFMO* in the analysis), nine of which are categorized as 'nc'. Group B contains a total of 63 splice variants pertaining to 57 genes, 14 of which are 'nc'. Lastly, Group C contains 80 splice variants pertaining to 74 genes, 16 of which are 'nc'.

replicates (Felsenstein, 1985). The tree figures were made with iTOL (Letunic and Bork, 2021).

We constructed separate ML phylogenies between all *TaFMO* and *FMO*s from closely-related species in the grass order, Poales—specifically, *H. vulgare* (barley), *T. urartu* (red einkorn wheat) and *O. sativa* ssp. japonica (rice) to improve our understanding of the relatedness of *TaFMO* in the three major clades A, B, and C (Supplementary Figures S2-5). For detailed notes on alignment and modelling, see Appendix S2.

2.4 Gene duplication and homeolog analysis, and protein motif analysis

We retrieved chromosomal locations of all *TaFMO*s in wheat from the RefSeqv2.1 gff3 file. We inferred homeologs based on well-supported phylogenetic clustering; separate sub-phylogenies were inferred for the three major partitions (clades A, B, and C) and a 70% bootstrap support value was used as a threshold to acknowledge clades with moderate support. Gene duplication and syntenic gene blocks of all *TaFMOs* (including 'nc' *TaFMOs*) were inferred through the MCSanX algorithm (Wang et al., 2012) via TBtools software v1.116 (Chen et al., 2022) and NOTUNG (Chen et al., 2000) to resolve tandem duplications and relationships between *TaFMO* homoeologous groups. Genes with no discernible relatives were denoted as 'orphan' *TaFMO* (Tables 2, 3). A comprehensive synchronized map of all *TaFMO* homeologs (Figure 3) connected by designated group colors assigned in Supplementary Figures S2-4 was generated using the shinyCircos software in RStudio (Yu et al., 2018; R Core Team, 2021). See Appendix S3 for more details. A *de novo* search for putative conserved protein motifs among all TaFMOs, HvFMOs, OsjFMOs, AtFMOs, AmTriFMOs, and PpFMOs was conducted with MEME Suite (Bailey et al., 2015): see Appendix S4.

2.5 TaFMO promoter regulatory elements analysis and transposable element identification

We searched promoter regions 1.5 kb upstream from the start codon of validated *TaFMOs* for plant *cis*-acting regulatory elements (PlantCARE: http://bioinformatics.psb.ugent.be/webtools/plantcare/html/; Lescot, 2002) and visualized putative cis-acting regulatory elements (CAREs) governing the different clades of *TaFMOs* (Supplementary Tables S3, 4, Appendix S5). We also compiled a list of putative transposable elements (TEs) detected by the CLARI-TE program (https://github.com/jdaron/CLARI-TE) either spanning introns and exons of *TaFMOs*, or flanking *TaFMOs* within a 2 kb region on either side (Table 4), from the TE annotation file provided in IWGSC RegSeqv2.1 (International Wheat Genome Sequencing Consortium et al., 2018; Zhu et al., 2021). The TE positions flanking or inside genes were transposed into *TaFMO* gene structure analysis. Refer to Appendix S6 for details.

2.6 Transcriptome, proteome, and tissue localization data retrieval and display

Using public transcriptomic data across a range of conditions, we extracted candidate *TaFMO* gene expression information, obtaining transcript values in FPKM for five general tissues (root, stem, leaves, spike, and grain) and proteome data (peptide spectral counts) for different tissues from the developmental atlas in the Wheat Proteome database (Duncan et al., 2017). We acquired transcript data for a broad range of different conditions in values of $\log_2$ transcripts per million (tpm) for *TaFMO* expression under various abiotic stressors (cold, drought, heat) and biotic stressors (i.e., infection by *Septoria blotch, Fusarium graminearum*, or *Puccinia striiformis* f.sp. *tritici*) from the Wheat Expression Database (Ramírez-González et al., 2018) in order to survey the differential expression of *TaFMO* candidates, and infer their possible biological functions (see Supplementary Tables S5-8 for an overview of studies and sources used).

3 Results and discussion

3.1 FMOs are a largely expanded gene family in flowering plants

The *FMO* gene family is highly expanded in the vascular plants, as previously reported (Eswaramoorthy et al., 2006; Mishina and Zeier, 2006; Schlaich, 2007; Thodberg and Jakobsen Neilson, 2020). Figure 1 exhibits the general number of potential FMO protein-encoding genes among select vascular plant reference genomes. The three most commonly present types of domain architectures that represent these plant FMOs are a single FMO-like domain (FMO-like), two consecutive FMO-like domains (FMO-like x 2), and a pyruvate redox 3 (Pyr3) domain. Some FMOs are predicted as fusion proteins, such as found in both wheat (*Ta*) and barley (*Hv*) with a tyrosine protein kinase conjugated to an FMO, alluding to a possible function in environmental sensing and downstream signaling coupled with oxidation processes (Tichtinsky et al., 2003; Shumayla and Upadhyay, 2023). The phenomenon of FMO fusion proteins does not present for lycophytes, moss, or algae, where total numbers of *FMOs* in the genome are substantially reduced relative to flowering vascular plant species. The total number of *FMOs* in plant genomes also appears to be largely reflective of species ploidy levels for recently diverged taxa, as exemplified in *Triticum urartu* (2n, 41 putative *TuFMOs*), *T. dicoccoides* (4n, 84 putative *TdFMOs*) and *T. aestivum* (6n, 170 putative *TaFMOs*). However, in plants considered diploid, the number of *FMOs* varies substantially, such as in *Arabidopsis* (29 *AtFMOs*), rice (31 *OsjFMOs*), and barley (59 *HvFMOs*), up to 64 potential *FMOs* in sunflower (*H. annuus*), which has double the amount of most diploid species in the eudicots (lower, green clade in Figure 1). We report several additional *FMO* candidates for rice compared to a recent report of 28 *OsjFMOs* by (Gaba et al., 2023), and for barley previously reported having 41 *HvFMOs* (Thodberg and Jakobsen Neilson, 2020), highlighting the complexity of conducting genome-wide searches for highly expanded gene families.

TABLE 2 TaFMO Homeolog analysis and literature evidence.

Group	TaFMO Sub-clade	Gene name	Possible roles	Citation	Synteny status	Chromosome	Triad status (A/B/D)	Triad status (ratio)
A	A1-Orphan	TraesCS7D03G1006000.1	Not Available	Not Available	Tandem (splice variant to TraesCS7D03G1006000.2)	7	-/-/D	Orphans/ singletons
		TraesCS7D03G1006000.2	Not Available	Not Available	Tandem (splice variant to TraesCS7D03G1006000.1)			
	A1-1	TraesCS5B03G0517200.1	Not Available	Not Available	Dispersed (from TraesCS5B03G0762600.1-nc)	5	A(Adis)/b (Btan) (Btan) (Bdis)/-	Other
		TraesCS5B03G0762600.1-nc	Not Available	Not Available	WGD or Segmental			
		TraesCS5A03G0725400.1	Not Available	Not Available	WGD or Segmental			
		TraesCS5B03G1289600.1	total tiller number increase; auxin biosynthesis and annotated as a 'YUCCA', in Group A[1]	[1] Vitale, P., Fania, F., Esposito, S., Pecorella, I., Pecchioni, N., Palombieri, S., Sestili, F., Lafiandra, D., Taranto, F., & De Vita, P. (2021). QTL Analysis of Five Morpho-Physiological Traits in Bread Wheat Using Two Mapping Populations Derived from Common Parents. Genes, 12(4), 604. https://doi.org/10.3390/genes12040604	Tandem (to TraesCS5B03G1289700.1)			
		TraesCS5B03G1289700.1	drought stress tolerance in roots[2]	[2] Grzesiak, M. T., Hordyńska, N., Maksymowicz, A., Grzesiak, S., & Szechyńska-Hebda, M. (2019). Variation Among Spring Wheat (Triticum aestivum L.) Genotypes in Response to the Drought Stress. II—Root System Structure. Plants, 8(12), 584. https://doi.org/10.3390/plants8120584	Tandem (to TraesCS5B03G1289600.1)			
		TraesCS5A03G1221300.1	Not Available	Not Available	Dispersed (from TraesCS5A03G0725400.1)			
	A1-2a	TraesCS4B03G0715800.1	Not Available	Not Available	WGD or Segmental	4	-/B/D	1 : 1 : 0/1 : 0 : 1/0 : 1 : 1
		TraesCS4D03G0639900.1	drought stress tolerance in roots[2]; amylose-lipid gelatinization[3]	[2] Grzesiak, M. T., Hordyńska, N., Maksymowicz, A., Grzesiak, S., & Szechyńska-Hebda, M. (2019). Variation Among Spring Wheat (Triticum aestivum L.) Genotypes in Response to the Drought Stress. II—Root System Structure. Plants, 8(12), 584. https://doi.org/10.3390/plants8120584; [3] Rahim, M. S., Kumar, V., & Roy, J. (2022). Genetic dissection of quantitative traits loci identifies new genes for gelatinization parameters of starch and amylose-lipid complex (Resistant starch 5) in bread wheat. Plant Science, 325, 111452. https://doi.org/10.1016/j.plantsci.2022.111452	WGD or Segmental			

(Continued)

10.3389/fpls.2024.1369299

TABLE 2 Continued

Group	TaFMO Sub-clade	Gene name	Possible roles	Citation	Synteny status	Chromosome	Triad status (A/B/D)	Triad status (ratio)
		TraesCS3D03G0019300.1	Not Available		WGD or Segmental	3	A/B(Btan)/D	n : 1 : 1/1 : n : 1/1 : 1 : n
		TraesCS3A03G0023200.1	drought stress tolerance in roots[2]	[2] Grzesiak, M. T., Hordyńska, N., Maksymowicz, A., Grzesiak, S., & Szechyńska-Hebda, M. (2019). Variation Among Spring Wheat (Triticum aestivum L.) Genotypes in Response to the Drought Stress. II—Root System Structure. Plants, 8(12), 584. https://doi.org/10.3390/plants8120584	WGD or Segmental			
		TraesCS3B03G0026700.1	Ni plant stress accumulation / metal stress in wheat plant[4]	[4] Safdar, L. B., Almas, F., Rehman, A. ur, Umer, M. J., Ali Shah, S. M., Uddin, S., Ashfaq, S., Rahman, H. U., & Quraishi, U. M. (2020). Genetic dissection of Ni toxicity in a spring wheat diversity panel by using 90 K SNP array. Current Plant Biology, 24, 100175. https://doi.org/10.1016/j.cpb.2020.100175	WGD or Segmental			
		TraesCS3B03G0026700.2			WGD or Segmental			
		TraesCS3B03G0026800.1	Not Available	Not Available	Tandem (to TraesCS3B03G0026700)			
		TraesCS3B03G0026800.2	Not Available	Not Available	Tandem (to TraesCS3B03G0026700)			
	A1-2b	TraesCS6B03G0454600.1	Not Available	Not Available	WGD or Segmental	6	a/B/-	1 : 1 : 0/1 : 0 : 1/0 : 1 : 1
		TraesCS6A03G0359800.1-nc	Not Available	Not Available	WGD or Segmental			
		TraesCS1B03G0013500.1	Not Available	Not Available	Proximal (to TraesCS1B03G0013100.1)	1	-/B(Btan)/-	Orphans/ singletons
		TraesCS1B03G0013100.1	Not Available	Not Available	Tandem (splice variant to TraesCS1B03G0013100.2)			
		TraesCS1B03G0013100.2-nc	Not Available	Not Available	Tandem (splice variant to TraesCS1B03G0013100.1)			
		TraesCS6B03G0373000.1	Not Available	Not Available	WGD or Segmental	6	A/B/D (Dprox)Un	n : 1 : 1/1 : n : 1/1 : 1 : n
		TraesCS6A03G0284300.1	Not Available	Not Available	WGD or Segmental			

(Continued)

10.3389/fpls.2024.1369299

TABLE 2 Continued

Group	TaFMO Sub-clade	Gene name	Possible roles	Citation	Synteny status	Chromosome	Triad status (A/B/D)	Triad status (ratio)
		TraesCS6A03G0284300.2	Not Available	Not Available	Tandem (splice variant to TraesCS6A03G0284300.1)			
		TraesCS6D03G0239900.1	Not Available	Not Available	Proximal (to TraesCS6D03G0239400)			
		TraesCS6D03G0239400.1	Not Available	Not Available	WGD or Segmental			
		TraesCSU03G0085200.1	Not Available	Not Available	Tandem (related to TraesCS6D03G0239400.1)			
		TraesCSU03G0085200.2	Not Available	Not Available				
		TraesCSU03G0085200.3	Not Available	Not Available				
	A2-Orphan	TraesCS1D03G0536600.1-nc	Not Available	Not Available	WGD or Segmental	1	A/-/d	1 : 1 : 0/1 : 0 : 1/0 : 1 : 1
		TraesCS1A03G0556900.1	drought stress tolerance in roots[2]	[2] Grzesiak, M. T., Hordyńska, N., Maksymowicz, A., Grzesiak, S., & Szechyńska-Hebda, M. (2019). Variation Among Spring Wheat (Triticum aestivum L.) Genotypes in Response to the Drought Stress. II—Root System Structure. Plants, 8(12), 584. https://doi.org/10.3390/plants8120584	WGD or Segmental			
	A2α-1	TraesCS1A03G0555700.1-nc	Not Available	Not Available	WGD or Segmental	1	a/B/D	1 : 1 : 1
		TraesCS1B03G0648500.1	Not Available	Not Available	WGD or Segmental			
		TraesCS1B03G0648500.2	Not Available	Not Available	Tandem (splice variant to TraesCS1B03G0648500.1)			
		TraesCS1B03G0648500.3	Not Available	Not Available				
		TraesCS1D03G0535600.1	Not Available	Not Available	WGD or Segmental			
		TraesCS1D03G0535600.2	Not Available	Not Available	Tandem (splice variant to TraesCS1D03G0535600.1)			
		TraesCS1D03G0535600.3	Not Available	Not Available				
	A2β-2	TraesCS6A03G0358100.1-nc	Not Available	Not Available	WGD or Segmental	6	a/-/D	1 : 1 : 0/1 : 0 : 1/0 : 1 : 1
		TraesCS6D03G0313400.1	Not Available	Not Available	WGD or Segmental			

(Continued)

10.3389/fpls.2024.1369299

TABLE 2 Continued

Group	TaFMO Sub-clade	Gene name	Possible roles	Citation	Synteny status	Chromosome	Triad status (A/B/D)	Triad status (ratio)
		TraesCS6D03G0313400.2	Not Available	Not Available	Tandem (splice variant to TraesCS6D03G0313400.1)			
		TraesCS6D03G0313400.3	Not Available	Not Available				
		TraesCS6D03G0313400.4	Not Available	Not Available				
	A2β-3	TraesCS4B03G0953400.1	Not Available	Not Available	Dispersed (from TraesCS4B03G0953300 and TraesCS4B03G0953000.1)	5 and 4	5A(aprox)/ 4BB(Bdis)/ 4D (Dtan)(dtan)	Other
		TraesCS4D03G0827700.1-nc	Not Available	Not Available	Tandem (to TraesCS4D03G0827800.1 and TraesCS4D03G0827900.1)			
		TraesCS4D03G0827700.2-nc	Not Available	Not Available				
		TraesCS4D03G0827900.1	Not Available	Not Available	WGD or Segmental: triad with TraesCS5A03G1253300.1, which was so truncated it wasn't included in the study.			
		TraesCS4B03G0953000.1	drought stress tolerance in roots[2]	[2] Grzesiak, M. T., Hordyńska, N., Maksymowicz, A., Grzesiak, S., & Szechyńska-Hebda, M. (2019). Variation Among Spring Wheat (Triticum aestivum L.) Genotypes in Response to the Drought Stress. II—Root System Structure. Plants, 8(12), 584. https://doi.org/10.3390/plants8120584	WGD or Segmental: triad with TraesCS5A03G1253300.1, which was so truncated it wasn't included in the study.			
		TraesCS5A03G1254200.1-nc	Not Available	Not Available	Proximal (possibly proximal to TraesCS5A03G1253300.1)			
		TraesCS4B03G0953300.1	Fg response in resistant wheat lines[5]	[5] Nussbaumer, T., Warth, B., Sharma, S., Ametz, C., Bueschl, C., Parich, A., Pfeifer, M., Siegwart, G., Steiner, B., Lemmens, M., Schuhmacher, R., Buerstmayr, H., Mayer, K. F. X., Kugler, K. G., & Schweiger, W. (2015). Joint Transcriptomic and Metabolomic Analyses Reveal Changes in the Primary Metabolism and Imbalances in the Subgenome Orchestration in the Bread Wheat Molecular Response to Fusarium graminearum. G3 Genes|Genomes|Genetics, 5(12), 2579–2592. https://doi.org/10.1534/g3.115.021550	WGD or Segmental			

(Continued)

10.3389/fpls.2024.1369299

TABLE 2 Continued

Group	TaFMO Sub-clade	Gene name	Possible roles	Citation	Synteny status	Chromosome	Triad status (A/B/D)	Triad status (ratio)
		TraesCS4D03G0827800.1	drought stress tolerance in roots[2]; Fg response in resistant wheat[5] lines[5]	[2] Grzesiak, M. T., Hordyńska, N., Maksymowicz, A., Grzesiak, S., & Szechyńska-Hebda, M. (2019). Variation Among Spring Wheat (Triticum aestivum L.) Genotypes in Response to the Drought Stress. II—Root System Structure. Plants, 8(12), 584. https://doi.org/10.3390/plants8120584; [5] Nussbaumer, T., Warth, B., Sharma, S., Ametz, C., Bueschl, C., Parich, A., Pfeifer, M., Siegwart, G., Steiner, B., Lemmens, M., Schuhmacher, R., Buerstmayr, H., Mayer, K. F. X., Kugler, K. G., & Schweiger, W. (2015). Joint Transcriptomic and Metabolomic Analyses Reveal Changes in the Primary Metabolism and Imbalances in the Subgenome Orchestration in the Bread Wheat Molecular Response to Fusarium graminearum. G3 Genes|Genomes|Genetics, 5(12), 2579–2592. https://doi.org/10.1534/g3.115.021550	Tandem (to TraesCS4D03G0827900 and TraesCS4D03G0827700.1-nc)			
		TraesCS5A03G1254100.1	Fg response in resistant wheat lines[5]	[5] Nussbaumer, T., Warth, B., Sharma, S., Ametz, C., Bueschl, C., Parich, A., Pfeifer, M., Siegwart, G., Steiner, B., Lemmens, M., Schuhmacher, R., Buerstmayr, H., Mayer, K. F. X., Kugler, K. G., & Schweiger, W. (2015). Joint Transcriptomic and Metabolomic Analyses Reveal Changes in the Primary Metabolism and Imbalances in the Subgenome Orchestration in the Bread Wheat Molecular Response to Fusarium graminearum. G3 Genes|Genomes|Genetics, 5(12), 2579–2592. https://doi.org/10.1534/g3.115.021550	WGD or Segmental			
		TraesCS5A03G1254100.2						
		TraesCS4B03G0947100.1	drought stress tolerance in roots[2]	[2] Grzesiak, M. T., Hordyńska, N., Maksymowicz, A., Grzesiak, S., & Szechyńska-Hebda, M. (2019). Variation Among Spring Wheat (Triticum aestivum L.) Genotypes in Response to the Drought Stress. II—Root System Structure. Plants, 8(12), 584. https://doi.org/10.3390/plants8120584	WGD or Segmental		5A/4B/-	1 : 1 : 0/1 : 0 : 1/0 : 1 : 1
		TraesCS5A03G1248100.1	drought stress tolerance in roots[2]; positively to helping plant against dual stress of heat + pathogen (spot blotch)	[2] Grzesiak, M. T., Hordyńska, N., Maksymowicz, A., Grzesiak, S., & Szechyńska-Hebda, M. (2019). Variation Among Spring Wheat (Triticum aestivum L.) Genotypes in Response to the Drought Stress. II—Root System Structure. Plants, 8(12), 584. https://doi.org/10.3390/plants8120584; [6] Navathe, S., Pandey, A. K., Sharma, S., Chand, R., Mishra, V. K., Kumar, D., Jaiswal, S., Iquebal, M. A., Govindan, V., Joshi, A. K., & Singh, P. K. (2022). New Genomic Regions Identified for Resistance to Spot Blotch and Terminal Heat Stress in an Interspecific Population of Triticum aestivum and T. spelta. Plants, 11(21), 2987. https://doi.org/10.3390/plants11212987	WGD or Segmental			

(Continued)

10.3389/fpls.2024.1369299

TABLE 2 Continued

Group	TaFMO Sub-clade	Gene name	Possible roles	Citation	Synteny status	Chromosome	Triad status (A/B/D)	Triad status (ratio)
B	B1-1	TraesCS4D03G0703600.1	Not Available	Not Available	Proximal	4	A/B(Btan) (udis) (udis)/ Dprox	n : 1 : 1/1 : n : 1/1 : 1 : n
		TraesCS4A03G0010700.1	Not Available	Not Available	WGD or Segmental			
		TraesCS4B03G0784200.1	Not Available	Not Available	WGD or Segmental			
		TraesCS4B03G0784300.1	Not Available	Not Available	Tandem (to TraesCS4B03G0784200.1)			
		TraesCSU03G0407900.1-nc	Not Available	Not Available	Dispersed			
		TraesCSU03G0436400.1-nc	Not Available	Not Available	Dispersed			
	B1-2a	TraesCS4B03G0783600.1	Not Available	Not Available	WGD or Segmental		A/B/D	1 : 1 : 1
		TraesCS4D03G0703400.1	Not Available	Not Available	Tandem			
		TraesCS4A03G0011000.1	Not Available	Not Available	WGD or Segmental			
	B1-2b	TraesCS4B03G0782700.1-nc	Not Available	Not Available	WGD or Segmental (synteny with TraesCS4A03G0011200.1)		A(Atan) (Atan)/b (Btan) (Btan)/D (Dtan) (Dtan)	1 : 1 : 1
		TraesCS4D03G0702600.1	Not Available	Not Available	WGD or Segmental			
		TraesCS4B03G0783000.1	Not Available	Not Available	Tandem to TraesCS4B03G0782700.1-nc			
		TraesCS4B03G0783300.1	Not Available	Not Available	Tandem to TraesCS4B03G0782700.1-nc			
		TraesCS4D03G0703000.1	Not Available	Not Available	Tandem to TraesCS4D03G0702600.1			
		TraesCS4D03G0702900.1	Not Available	Not Available	Tandem to TraesCS4D03G0702600.1			
		TraesCS4D03G0702900.2	Not Available	Not Available				

(Continued)

10.3389/fpls.2024.1369299

TABLE 2 Continued

Group	TaFMO Sub-clade	Gene name	Possible roles	Citation	Synteny status	Chromosome	Triad status (A/B/D)	Triad status (ratio)
		TraesCS4A03G0011100.1	Not Available	Not Available	Tandem (to TraesCS4A03G0011200.1)			
		TraesCS4A03G0011200.1	Not Available	Not Available	WGD or Segmental			
		TraesCS4A03G0011700.1	Not Available	Not Available	Tandem (to TraesCS4A03G0011200.1)			
	B2α-1	TraesCS5D03G0802100.1-nc	Not Available	Not Available	WGD or Segmental	5	A/B/ d(Dtan)	n : 1 : 1/1 : n : 1/1 : 1 : n
		TraesCS5A03G0839400.1	drought stress tolerance in roots[2]	[2] Grzesiak, M. T., Hordyńska, N., Maksymowicz, A., Grzesiak, S., & Szechyńska-Hebda, M. (2019). Variation Among Spring Wheat (Triticum aestivum L.) Genotypes in Response to the Drought Stress. II—Root System Structure. Plants, 8(12), 584. https://doi.org/10.3390/plants8120584	WGD or Segmental			
		TraesCS5B03G0877300.1	drought stress tolerance in roots[2]; seminal root growth (TaFMO1-5B)[8]	[2] Grzesiak, M. T., Hordyńska, N., Maksymowicz, A., Grzesiak, S., & Szechyńska-Hebda, M. (2019). Variation Among Spring Wheat (Triticum aestivum L.) Genotypes in Response to the Drought Stress. II—Root System Structure. Plants, 8(12), 584. https://doi.org/10.3390/plants8120584; [8]	WGD or Segmental			
		TraesCS5D03G0802200.1	drought stress tolerance in roots[2]	[2] Grzesiak, M. T., Hordyńska, N., Maksymowicz, A., Grzesiak, S., & Szechyńska-Hebda, M. (2019). Variation Among Spring Wheat (Triticum aestivum L.) Genotypes in Response to the Drought Stress. II—Root System Structure. Plants, 8(12), 584. https://doi.org/10.3390/plants8120584	Tandem (to TraesCS5D03G0802100.1-nc)			
	B2α-2	TraesCS5B03G0873900.1	ornithine biosynthesis[7]	[7] Matros, A., Liu, G., Hartmann, A., Jiang, Y., Zhao, Y., Wang, H., Ebmeyer, E., Korzun, V., Schachschneider, R., Kazman, E., Schacht, J., Longin, F., Reif, J. C., & Mock, H.-P. (2016). Genome–metabolite associations revealed low heritability, high genetic complexity, and causal relations for leaf metabolites in winter wheat (Triticum aestivum). Journal of Experimental Botany, erw441. https://doi.org/10.1093/jxb/erw441	Tandem (to TraesCS5B03G0873800.1)	5	A(Atan)/B (Btan)/ D(Dtan)	1 : 1 : 1 (2 triads tandem)
		TraesCS5D03G0799100.1	ornithine biosynthesis[7]	[7] Matros, A., Liu, G., Hartmann, A., Jiang, Y., Zhao, Y., Wang, H., Ebmeyer, E., Korzun, V., Schachschneider, R., Kazman, E., Schacht, J., Longin, F., Reif, J. C., & Mock, H.-P. (2016). Genome–metabolite associations revealed low heritability, high genetic complexity, and causal relations for leaf metabolites in winter wheat (Triticum aestivum).	Tandem (to TraesCS5D03G0798800.1)			

(Continued)

10.3389/fpls.2024.1369299

TABLE 2 Continued

Group	TaFMO Sub-clade	Gene name	Possible roles	Citation	Synteny status	Chromosome	Triad status (A/B/D)	Triad status (ratio)
				Journal of Experimental Botany, erw441. https://doi.org/10.1093/jxb/erw441				
		TraesCS5A03G0836200.1	ornithine biosynthesis[7]; wheat leaf rust QTN loci for seedling resistance to WLR[9]	[7] Matros, A., Liu, G., Hartmann, A., Jiang, Y., Zhao, Y., Wang, H., Ebmeyer, E., Korzun, V., Schachschneider, R., Kazman, E., Schacht, J., Longin, F., Reif, J. C., & Mock, H.-P. (2016). Genome–metabolite associations revealed low heritability, high genetic complexity, and causal relations for leaf metabolites in winter wheat (Triticum aestivum). Journal of Experimental Botany, erw441. https://doi.org/10.1093/jxb/erw441; [9] Vikas, V. K., Pradhan, A. K., Budhlakoti, N., Mishra, D. C., Chandra, T., Bhardwaj, S. C., Kumar, S., Sivasamy, M., Jayaprakash, P., Nisha, R., Shajitha, P., Peter, J., Geetha, M., Mir, R. R., Singh, K., & Kumar, S. (2022). Multi-locus genome-wide association studies (ML-GWAS) reveal novel genomic regions associated with seedling and adult plant stage leaf rust resistance in bread wheat (Triticum aestivum L.). Heredity, 128(6), 434–449. https://doi.org/10.1038/s41437-022-00525-1	Tandem (to TraesCS5A03G0836000.1)			
		TraesCS5B03G0873800.1	ornithine biosynthesis[7]	[7] Matros, A., Liu, G., Hartmann, A., Jiang, Y., Zhao, Y., Wang, H., Ebmeyer, E., Korzun, V., Schachschneider, R., Kazman, E., Schacht, J., Longin, F., Reif, J. C., & Mock, H.-P. (2016). Genome–metabolite associations revealed low heritability, high genetic complexity, and causal relations for leaf metabolites in winter wheat (Triticum aestivum). Journal of Experimental Botany, erw441. https://doi.org/10.1093/jxb/erw441	WGD or Segmental			
		TraesCS5D03G0798800.1	ornithine biosynthesis[7]	[7] Matros, A., Liu, G., Hartmann, A., Jiang, Y., Zhao, Y., Wang, H., Ebmeyer, E., Korzun, V., Schachschneider, R., Kazman, E., Schacht, J., Longin, F., Reif, J. C., & Mock, H.-P. (2016). Genome–metabolite associations revealed low heritability, high genetic complexity, and causal relations for leaf metabolites in winter wheat (Triticum aestivum). Journal of Experimental Botany, erw441. https://doi.org/10.1093/jxb/erw441	WGD or Segmental			
		TraesCS5A03G0836000.1	ornithine biosynthesis[7]	[7] Matros, A., Liu, G., Hartmann, A., Jiang, Y., Zhao, Y., Wang, H., Ebmeyer, E., Korzun, V., Schachschneider, R., Kazman, E., Schacht, J., Longin, F., Reif, J. C., & Mock, H.-P. (2016). Genome–metabolite associations revealed low heritability, high genetic complexity, and causal relations for leaf metabolites in winter wheat (Triticum aestivum).	WGD or Segmental			

(Continued)

10.3389/fpls.2024.1369299

TABLE 2 Continued

Group	TaFMO Sub-clade	Gene name	Possible roles	Citation	Synteny status	Chromosome	Triad status (A/B/D)	Triad status (ratio)
				Journal of Experimental Botany, erw441. https://doi.org/10.1093/jxb/erw441				
	B2β-3a	TraesCS5B03G0875600.1	Not Available	Not Available	WGD or Segmental	5	A/B/D	1 : 1 : 1
		TraesCS5B03G0875600.2	Not Available	Not Available	Tandem (to TraesCS5B03G0875600.1)			
		TraesCS5D03G0799800.1	Not Available	Not Available	WGD or Segmental			
		TraesCS5A03G0837700.1	Not Available	Not Available	WGD or Segmental			
	B2β-3b	TraesCS5D03G0450200.1-nc	Not Available	Not Available	WGD or Segmental (synteny with TraesCS5A03G0486900.1 and TraesCS5B03G0485700.1)	5	A/B/d (ddis) (dprox)	n : 1 : 1/1 : n : 1/1 : 1 : n
		TraesCS5B03G0485700.1	Not Available	Not Available	WGD or Segmental			
		TraesCS5D03G0450600.1-nc	Not Available	Not Available	Dispersed (tandem to TraesCS5D03G0450200.1-nc)			
		TraesCS5D03G0450700.1-nc	Not Available	Not Available	Proximal (tandem to TraesCS5D03G0450200.1-nc)			
		TraesCS5A03G0486900.1	Not Available	Not Available	WGD or Segmental			
	B2β-4a	TraesCS2D03G0137200.1	Not Available	Not Available	WGD or Segmental	2	A/B (Bprox)/D	n : 1 : 1/1 : n : 1/1 : 1 : n
		TraesCS2A03G0138700.1	possibly involved in spot blotch disease (significantly enriched SNP); PREPRINT ONLY	See Supplementary Table S6	WGD or Segmental			
		TraesCS2B03G0193300.1	Not Available	Not Available	WGD or Segmental			
		TraesCS2B03G0193600.1	Not Available	Not Available	Proximal (to TraesCS2B03G0193300.1)			
	B2β-4b	TraesCS1D03G0254900.1	Not Available	Not Available	WGD or Segmental	1	A/-/D	1 : 1 : 0/1 : 0 : 1/0 : 1 : 1
		TraesCS1A03G0258900.1	Not Available	Not Available	WGD or Segmental			

(Continued)

10.3389/fpls.2024.1369299

TABLE 2 Continued

Group	TaFMO Sub-clade	Gene name	Possible roles	Citation	Synteny status	Chromosome	Triad status (A/B/D)	Triad status (ratio)
		TraesCS1A03G0258900.2	Not Available	Not Available	Tandem			
	B2β-4c(1)	TraesCS2A03G0138800.1	possibly involved in spot blotch disease (significantly enriched SNP); PREPRINT ONLY	See Supplementary Table S6	WGD or Segmental	2	A/B(bBbB) tan/D	n : 1 : 1/1 : n : 1/1 : 1 : n
		TraesCS2D03G0137800.1	Not Available	Not Available	WGD or Segmental			
		TraesCS2B03G0193800.1	Not Available	Not Available	WGD or Segmental			
		TraesCS2B03G0194000.1-nc	Not Available	Not Available	Tandem (to TraesCS2B03G0193800.1)			
		TraesCS2B03G0194300.1	Not Available	Not Available	Tandem (to TraesCS2B03G0193800.1)			
		TraesCS2B03G0194100.1	Not Available	Not Available	Tandem (to TraesCS2B03G0193800.1)			
		TraesCS2B03G0194200.1-nc	Not Available	Not Available	Tandem (to TraesCS2B03G0193800.1)			
	B2β-4c(2)	TraesCS7D03G1269100.1	drought stress tolerance in roots[2]	[2] Grzesiak, M. T., Hordyńska, N., Maksymowicz, A., Grzesiak, S., & Szechyńska-Hebda, M. (2019). Variation Among Spring Wheat (Triticum aestivum L.) Genotypes in Response to the Drought Stress. II—Root System Structure. Plants, 8(12), 584. https://doi.org/10.3390/plants8120584	WGD or Segmental (TraesCS7A03G1341700.1 and TraesCS7B03G1279000.1)	7	A(atan)/B (bprox) (Bdis) (udis)/DD	Other
		TraesCS7B03G1279500.1	stem rust resistance: resposive to Pgt at 96hpi in wheat[11]	[11] Sahu, R., Prabhakaran, N., Kundu, P., & Kumar, A. (2021). Differential response of phytohormone signalling network determines nonhost resistance in rice during wheat stem rust (Puccinia graminis f. Sp. Tritici) colonization. Plant Pathology, 70(6), 1409–1420. https://doi.org/10.1111/ppa.13376	Dispersed			
		TraesCS7D03G1268300.1	drought stress tolerance in roots[2]	[2] Grzesiak, M. T., Hordyńska, N., Maksymowicz, A., Grzesiak, S., & Szechyńska-Hebda, M. (2019). Variation Among Spring Wheat (Triticum aestivum L.) Genotypes in Response to the Drought Stress. II—Root System Structure. Plants, 8(12), 584. https://doi.org/10.3390/plants8120584	WGD or Segmental			
		TraesCS7D03G1268300.2-nc						
		TraesCS7A03G1341700.1	total tiller number increase; auxin biosynthesis[1];	[1] Vitale, P., Fania, F., Esposito, S., Pecorella, I., Pecchioni, N., Palombieri, S., Sestili, F., Lafiandra, D., Taranto, F., & De	WGD or Segmental			

(Continued)

10.3389/fpls.2024.1369299

TABLE 2 Continued

Group	TaFMO Sub-clade	Gene name	Possible roles	Citation	Synteny status	Chromosome	Triad status (A/B/D)	Triad status (ratio)
			drought stress tolerance in roots[2]; possibly barley yellow dwarf virus resistance (PhD THESIS)	Vita, P. (2021). QTL Analysis of Five Morpho-Physiological Traits in Bread Wheat Using Two Mapping Populations Derived from Common Parents. Genes, 12(4), 604. https://doi.org/10.3390/genes12040604; [2] Grzesiak, M. T., Hordyńska, N., Maksymowicz, A., Grzesiak, S., & Szechyńska-Hebda, M. (2019). Variation Among Spring Wheat (Triticum aestivum L.) Genotypes in Response to the Drought Stress. II—Root System Structure. Plants, 8(12), 584. https://doi.org/10.3390/plants8120584; See Supplementary Table S6				
		TraesCS7A03G1341700.2-nc						
		TraesCS7A03G1342300.1-nc	possibly barley yellow dwarf virus resistance (PhD THESIS)	See Supplementary Table S6	WGD or Segmental			
		TraesCS7B03G1279000.1	Not Available	Not Available	WGD or Segmental			
		TraesCS7B03G1279000.2	Not Available	Not Available	WGD or Segmental			
		TraesCS7B03G1279300.1-nc	Not Available	Not Available	Proximal			
		TraesCSU03G0348300.1-nc	Not Available	Not Available	Dispersed			
C	C1-1	TraesCS4A03G0051300.1	Not Available	Not Available	WGD or Segmental	4	A/B/D	1 : 1 : 1
		TraesCS4D03G0656000.1	Not Available	Not Available	WGD or Segmental			
		TraesCS4B03G0738000.1	Not Available	Not Available	WGD or Segmental			
	C1-2a	TraesCS5B03G1370600.1	Not Available	Not Available	WGD or Segmental	4 and 5	4A / 5B / -	1 : 1 : 0/1 : 0 : 1/0 : 1 : 1
		TraesCS4A03G0782000.1	drought stress tolerance in roots[2]	[2] Grzesiak, M. T., Hordyńska, N., Maksymowicz, A., Grzesiak, S., & Szechyńska-Hebda, M. (2019). Variation Among Spring Wheat (Triticum aestivum L.) Genotypes in Response to the Drought Stress. II—Root System Structure. Plants, 8(12), 584. https://doi.org/10.3390/plants8120584	WGD or Segmental			
	C1-2b	TraesCS2A03G0024200.1	drought stress tolerance in roots[2]; AtYUCCA9-like; with a TM domain and expressed more highly in	[2] Grzesiak, M. T., Hordyńska, N., Maksymowicz, A., Grzesiak, S., & Szechyńska-Hebda, M. (2019). Variation Among Spring Wheat (Triticum aestivum L.) Genotypes in Response to the Drought Stress. II—Root System Structure.	WGD or Segmental	2	A/B/D	1 : 1 : 1

(Continued)

10.3389/fpls.2024.1369299

TABLE 2 Continued

Group	TaFMO Sub-clade	Gene name	Possible roles	Citation	Synteny status	Chromosome	Triad status (A/B/D)	Triad status (ratio)
			embryo sac cells relative to antipodal cells[16]	Plants, 8(12), 584. https://doi.org/10.3390/plants8120584; [16] Doronina, T. V., Ashapkin, V. V., & Lazareva, E. M. (2022). Wheat Antipodal Cells with Polytene Chromosomes in the Embryo Sac Are Key to Understanding the Formation of Grain in Cereals. Biology, 11(9), 1340. https://doi.org/10.3390/biology11091340				
		TraesCS2D03G0022100.1	drought stress tolerance in roots[2]	[2] Grzesiak, M. T., Hordyńska, N., Maksymowicz, A., Grzesiak, S., & Szechyńska-Hebda, M. (2019). Variation Among Spring Wheat (Triticum aestivum L.) Genotypes in Response to the Drought Stress. II—Root System Structure. Plants, 8(12), 584. https://doi.org/10.3390/plants8120584	WGD or Segmental			
		TraesCS2B03G0030700.2	drought stress tolerance in roots[2]	[2] Grzesiak, M. T., Hordyńska, N., Maksymowicz, A., Grzesiak, S., & Szechyńska-Hebda, M. (2019). Variation Among Spring Wheat (Triticum aestivum L.) Genotypes in Response to the Drought Stress. II—Root System Structure. Plants, 8(12), 584. https://doi.org/10.3390/plants8120584	Tandem (splice to TraesCS2B03G0030700.1)			
		TraesCS2B03G0030700.1	Not Available	Not Available	WGD or Segmental			
	C1-2b-orphan	TraesCS7D03G0088000.1	Not Available	Not Available	WGD or Segmental	7	-/-/Du.	Orphans/ singletons
		TraesCSU03G0061100.1-nc	Not Available	Not Available	WGD or Segmental			
	C1-2b(1)	TraesCS2A03G1234200.1	linked with higher H2O2 content under drought stress[13]	[13] Kamruzzaman, M., Beyene, M. A., Siddiqui, M. N., Ballvora, A., Léon, J., & Naz, A. A. (2022). Pinpointing genomic loci for drought-induced proline and hydrogen peroxide accumulation in bread wheat under field conditions. BMC Plant Biology, 22(1), 584. https://doi.org/10.1186/s12870-022-03943-9	WGD or Segmental	2	A/B/D	1 : 1 : 1
		TraesCS2D03G1190900.1	Not Available	Not Available	WGD or Segmental			
		TraesCS2B03G1409100.1	Not Available	Not Available	WGD or Segmental			
	C1-3	TraesCS3D03G0553100.1	Not Available	Not Available	WGD or Segmental	3	A/B/D	1 : 1 : 1
		TraesCS3A03G0598600.1	Not Available	Not Available	WGD or Segmental			
		TraesCS3B03G0681000.1	Not Available	Not Available	WGD or Segmental			
	C1-4a	TraesCS5B03G0272800.1-nc	Not Available	Not Available	WGD or Segmental	5	A/b/D	1 : 1 : 1
		TraesCS5D03G0268800.1	Not Available	Not Available	WGD or Segmental			

(Continued)

10.3389/fpls.2024.1369299

TABLE 2 Continued

Group	TaFMO Sub-clade	Gene name	Possible roles	Citation	Synteny status	Chromosome	Triad status (A/B/D)	Triad status (ratio)
		TraesCS5A03G0261000.1	Not Available	Not Available	WGD or Segmental			
	C1-4b	TraesCS3B03G0422400.1	Not Available	Not Available	WGD or Segmental	3	A/B/D	1 : 1 : 1
		TraesCS3D03G0335700.1	Not Available	Not Available	WGD or Segmental			
		TraesCS3A03G0344800.1	downregulated at reproductive stage in drought stress[14]	[14] Samtani, H., Sharma, A., & Khurana, P. (2022). Overexpression of HVA1 Enhances Drought and Heat Stress Tolerance in Triticum aestivum Doubled Haploid Plants. Cells, 11(5), 912. https://doi.org/10.3390/cells11050912	WGD or Segmental			
	C1-4c	TraesCS3A03G0706200.1	Not Available	Not Available	WGD or Segmental	3	A/B/D	1 : 1 : 1
		TraesCS3D03G0648800.1	Not Available	Not Available	WGD or Segmental			
		TraesCS3B03G0807100.1	Not Available	Not Available	WGD or Segmental			
	C2-1	TraesCS7D03G0136300.1	Not Available	Not Available	WGD or Segmental	7	A/-/D	1 : 1 : 0/1 : 0 : 1/0 : 1 : 1
		TraesCS7A03G0147900.1	Not Available	Not Available	WGD or Segmental			
		TraesCS5A03G0560600.1	Not Available	Not Available	WGD or Segmental	5	A/B/D	1 : 1 : 1
		TraesCS5B03G0571000.1	QTL identified of 135 as possibly involved in grain content and quality[17]; expressed in the early uninucleate stage of a wheat MR (fertile near-isogenic) line in auxin biosynthesis pathway[18]; coexpression network analysis characterized TaYUCCA11-5B (TraesCS5B02G216000) as the central gene potentially responsible for the differential biosynthesis of auxin between Fe+NaCl and +Fe+NaCl conditions[19]	[17] Li, N., Miao, Y., Ma, J., Zhang, P., Chen, T., Liu, Y., Che, Z., Shahinnia, F., & Yang, D. (2023). Consensus genomic regions for grain quality traits in wheat revealed by meta-QTL analysis and in silico transcriptome integration. The Plant Genome, 16, e20336. https://doi.org/10.1002/tpg2.20336; [18] Wu, B., Xia, Y., Zhang, G., Wang, Y., Wang, J., Ma, S., Song, Y., Yang, Z., Ma, L., & Niu, N. (2023). Transcriptomics reveals a core transcriptional network of K-type cytoplasmic male sterility microspore abortion in wheat (Triticum aestivum L.). BMC Plant Biology, 23(1), 618. https://doi.org/10.1186/s12870-023-04611-2; [19] Hua, Y., Zhang, Y., Zhang, T., Chen, J., Song, H., Wu, P., Yue, C., Huang, J., Feng, Y., & Zhou, T. (2023). Low iron ameliorates the salinity-induced growth cessation of seminal roots in wheat seedlings. Plant, Cell & Environment, 46(2), 567–591. https://doi.org/10.1111/pce.14486	WGD or Segmental			
		TraesCS5D03G0526200.1	Not Available	Not Available	WGD or Segmental			

(Continued)

10.3389/fpls.2024.1369299

TABLE 2 Continued

Group	TaFMO Sub-clade	Gene name	Possible roles	Citation	Synteny status	Chromosome	Triad status (A/B/D)	Triad status (ratio)
	C2-2	TraesCS4A03G0924600.2	Not Available	Not Available	Tandem (splice to TraesCS4A03G0924600.1)	4 and 7	4A / 7A / 7D; translocation	1 : 1 : 1
		TraesCS4A03G0924600.1	Not Available	Not Available	WGD or Segmental			
		TraesCS7D03G0164500.1	Not Available	Not Available	WGD or Segmental			
		TraesCS7A03G0175600.1	total tiller number increase; auxin biosynthesis and annotated as a 'YUCCA'[1]	[1] Vitale, P., Fania, F., Esposito, S., Pecorella, I., Pecchioni, N., Palombieri, S., Sestili, F., Lafiandra, D., Taranto, F., & De Vita, P. (2021). QTL Analysis of Five Morpho-Physiological Traits in Bread Wheat Using Two Mapping Populations Derived from Common Parents. Genes, 12(4), 604. https://doi.org/10.3390/genes12040604	WGD or Segmental			
	C2-3	TraesCS5B03G1338800.1	TaYUCCA10.1[15]	[15] Li, N., Yin, N., Niu, Z., Hui, W., Song, J., Huang, C., Wang, H., Kong, L., & Feng, D. (2014). Isolation and characterization of three TaYUC10genes from wheat. Gene, 546(2), 187–194. https://doi.org/10.1016/j.gene.2014.06.020	WGD or Segmental	4, 5, and 6	4A / 5B / 5D(6Bdis)	n : 1 : 1/1 : n : 1/1 : 1 : n
		TraesCS5D03G1224400.1	TaYUCCA10.3[15]	[15] Li, N., Yin, N., Niu, Z., Hui, W., Song, J., Huang, C., Wang, H., Kong, L., & Feng, D. (2014). Isolation and characterization of three TaYUC10genes from wheat. Gene, 546(2), 187–194. https://doi.org/10.1016/j.gene.2014.06.020	WGD or Segmental			
		TraesCS6B03G0077300.1	Not Available	Not Available	Dispersed (not on synteny analysis; likely dispersed TraesCS5D03G1224400.1)			
		TraesCS5D03G1224400.3-nc	Not Available	Not Available	Tandem (splice variant to TraesCS5D03G1224400.1)			
		TraesCS5D03G1224400.2-nc	Not Available	Not Available	Tandem (splice variant to TraesCS5D03G1224400.1)			
		TraesCS4A03G0811300.1	Not Available	Not Available	WGD or Segmental			
		TraesCS4A03G0811300.2	Not Available	Not Available	Tandem (splice to TraesCS4A03G0811300.1)			
		TraesCS4A03G0811300.3	TaYUCCA10.2[15]	[15] Li, N., Yin, N., Niu, Z., Hui, W., Song, J., Huang, C., Wang, H., Kong, L., & Feng, D. (2014). Isolation and characterization of three TaYUC10genes from wheat. Gene, 546(2), 187–194. https://doi.org/10.1016/j.gene.2014.06.020	Tandem (splice to TraesCS4A03G0811300.1)			

(Continued)

10.3389/fpls.2024.1369299

TABLE 2 Continued

Group	TaFMO Sub-clade	Gene name	Possible roles	Citation	Synteny status	Chromosome	Triad status (A/B/D)	Triad status (ratio)
	C2-4a	TraesCS2D03G1263800.1-nc	Not Available	Not Available	WGD or Segmental (to TraesCS2A03G1299900.1-nc)	2	A(atan)/B/D (d) (dtan)(dtan)	Other
		TraesCS2D03G1263600.1	Not Available	Not Available	WGD or Segmental (to TraesCS2A03G1299700.1)			
		TraesCS2A03G1299700.1	Not Available	Not Available	WGD or Segmental (TraesCS2D03G1263600.1 + TraesCS2B03G1491700.1)			
		TraesCS2A03G1299600.1-nc	Not Available	Not Available	Tandem (clustered with TraesCS2A03G1299700.1)			
		TraesCS2A03G1299800.1	Not Available	Not Available	Tandem			
		TraesCS2A03G1300100.1	Not Available	Not Available	Tandem			
		TraesCS2A03G1299900.1-nc	Not Available	Not Available	WGD or Segmental (to TraesCS2D03G1263800.1-nc)			
		TraesCS2D03G1263400.1-nc	Not Available	Not Available	Tandem		a(Atan) (Atan)/B (Btan)(btan) (Btan)(Btan) (Udis)/d(d)	Other
		TraesCS2D03G1263300.1-nc	Not Available	Not Available	Tandem			
		TraesCS2D03G1263100.1-nc	Not Available	Not Available	WGD or Segmental			
		TraesCS2B03G1491700.1	Not Available	Not Available	WGD or Segmental			
		TraesCS2D03G1263200.1-nc	Not Available	Not Available	WGD or Segmental			
		TraesCSU03G0267700.1	Not Available	Not Available	Dispersed			
		TraesCS2B03G1490400.1-nc	Not Available	Not Available	Tandem			
		TraesCS2B03G1490600.1	Not Available	Not Available	Tandem			
		TraesCS2B03G1490500.1	Not Available	Not Available	Tandem			

(Continued)

10.3389/fpls.2024.1369299

TABLE 2 Continued

Group	TaFMO Sub-clade	Gene name	Possible roles	Citation	Synteny status	Chromosome	Triad status (A/B/D)	Triad status (ratio)
		TraesCS2B03G1490300.1	Not Available	Not Available	Tandem			
		TraesCS2B03G1490200.1	total tiller number increase; auxin biosynthesis and annotated as a 'YUCCA'[1]	[1] Vitale, P., Fania, F., Esposito, S., Pecorella, I., Pecchioni, N., Palombieri, S., Sestili, F., Lafiandra, D., Taranto, F., & De Vita, P. (2021). QTL Analysis of Five Morpho-Physiological Traits in Bread Wheat Using Two Mapping Populations Derived from Common Parents. Genes, 12(4), 604. https://doi.org/10.3390/genes12040604	WGD or Segmental			
	C2-4b	TraesCS7D03G0165100.1	Not Available	Not Available	WGD or Segmental	2, 4, and 7	Not Categorized‡	
		TraesCS4A03G0926100.1	Not Available	Not Available	WGD or Segmental			
		TraesCS2B03G1504900.1	Not Available	Not Available	Dispersed			
		TraesCS2B03G1502400.1	Not Available	Not Available	Dispersed			
		TraesCS4A03G0927400.1	Not Available	Not Available	Tandem (TraesCS4A03G0926600.1)			
		TraesCS7D03G0166500.1	Not Available	Not Available	Tandem (to TraesCS7D03G0166400.1-nc)			
		TraesCS7D03G0166400.1-nc	Not Available	Not Available	WGD or Segmental			
		TraesCS7A03G0177400.1	Not Available	Not Available	WGD or Segmental			
		TraesCS7A03G0177300.1	Not Available	Not Available	WGD or Segmental			
		TraesCS7A03G0177100.1-nc	Not Available	Not Available	Tandem (to both TraesCS7A03G0177300.1 and TraesCS7A03G0177400.1)			
		TraesCS7D03G0166200.1	Not Available	Not Available	Dispersed			
		TraesCS7D03G0165600.1	Not Available	Not Available	Dispersed			
		TraesCS7A03G1116400.1	Not Available	Not Available	Dispersed			
		TraesCS4A03G0926600.1	Not Available	Not Available	WGD or Segmental			
		TraesCS7A03G0176900.1-nc	Not Available	Not Available	WGD or Segmental			
		TraesCS4A03G0927300.1-nc	Not Available	Not Available	Tandem (TraesCS4A03G0926600.1)			

(Continued)

10.3389/fpls.2024.1369299

TABLE 2 Continued

Group	TaFMO Sub-clade	Gene name	Possible roles	Citation	Synteny status	Chromosome	Triad status (A/B/D)	Triad status (ratio)
		TraesCS7B03G0011300.1	Not Available	Not Available	Dispersed			
		TraesCS4A03G0943300.1-nc	Not Available	Not Available	Tandem			
		TraesCS4A03G0943200.1	Not Available	Not Available	Tandem			

An HMM search conducted against the RefSeqv2.1 wheat reference genome for cultivar 'Chinese Spring' yielded a total of 171 high confidence (HC) *TaFMO* genes, and 82 low confidence (LC) *TaFMO* genes. We selected 170 HC *TaFMO* genes including those deemed 'unmapped' to specific chromosomes after consolidation with other search methods (see Supplementary Figure S1, Appendix S1 for additional information). A total of 34 *TaFMO* candidate genes (40 including transcript splice variants) are denoted as 'non-canonical' (nc), based on alterations in—or the absence of—protein motifs previously reported as crucial for proper FMO function, discussed below (Table 2). The 'nc' *TaFMO*s possessing alterations in important protein motifs but were still found in synteny with other *TaFMO* homoeologous triads, were retained in downstream analyses; further experimental validation is required to prove their functional and biological relevance as an FMO in wheat. Other more highly truncated 'nc' *TaFMOs* unlikely functional in the canonical sense, could still highlight trends in motif diversification/loss for certain subclades when included in a phylogenetic analysis. The same logic was applied to sort for FMOs of *Arabidopsis thaliana* (*At*), *Oryza sativa* ssp. japonica (*Osj*), *Hordeum vulgare* (*Hv*), and *Triticum urartu* (*Tu*).

3.2 TaFMOs are consistently divided into three major groups across vascular plants, and span all chromosomes and sub-genomes

A maximum-likelihood phylogeny was constructed with protein sequences representing the total 170 *TaFMO* gene candidates (198 independent splice variants); *FMO*s from *Amborella trichopoda* (*Amtri*), rice *Oryza sativa* sp. Japonica (*Osj*), and *A. thaliana* (*At*) were included to probe for phylogenetic partitioning of *TaFMOs* among flowering plants. A red microalgae (*G. sulphuraria*) served as an outgroup, whose genome encodes for only one known *FMO* (Figure 1). We observed three major phylogenetic groupings, indicated as A, B, and C in Figure 2.

Domain architecture analysis (Figure 2, circle I) shows that Group A FMOs mostly share the same domain architecture type as the FMO from the outgroup red algae ('FMO-like x 2'), with two TaFMOs as exceptions having the 'pyruvate redox 2' architecture (TraesCS3B03G0026700.1, TraesCS3B03G0026800.2). Group B (purple) and Group C (green) FMOs form a clade across vascular plants with Group B mostly composed of an 'FMO-like' architecture, whereas group C has a mix between the 'FMO-like' and 'pyruvate redox 3' architectures. The distribution of total FMOs across an array of vascular plants (or within one species) has been documented by Thodberg and Jakobsen Neilson (2020); Gaba et al. (2023), and Yoshimoto et al. (2015), and the phylogenies presented in these studies also find Group B (*AtFMO1*-containing clade) and Group C ('*YUCCA*' clade) to be more closely related to each other than to Group A (the *AtFMO GSOX*-containing clade).

We found that *TaFMOs* span all seven (and unmapped) chromosomes and sub-genomes (A, B, and D) derived from progenitor grass species *Triticum urartu*, *Aegilops speltoides*, and

Aegilops tauschii, respectively (Ramírez-González et al., 2018; Zhu et al., 2021). Chromosomes 2, 4 and 7 are enriched with *TaFMO*s in the telomeric regions (Figure 3). Translocations of *TaFMOs* are inferred to have occurred most frequently between chromosomes 4A, 7A, and 7D, which are reported to be hot spots for homoeologous gene translocation events for many genes in wheat (Zhou et al., 2020) (Appendix S3). Other prominent translocations of *TaFMO* occurred between chromosomes 4A, 5A, and 5B in Group C *TaFMO*, and between chromosomes 5A, 4B, and 4D in Group A *TaFMO* (Figure 3, Table 2).

3.3 Sub-groups reveal non-uniform patterns of TaFMO gene expansion

Tables 2, 3 summarize the synteny status of Groups A, B, and C *TaFMO* homeologs and homeolog sub-genome ratios (denoted as a *TaFMO* ratio of 1: 1: 1 from A, B, and D sub-genomes), respectively. Group A *TaFMOs* show substantially less syntenic triads with only 8.2% of triads in Group A exhibiting an even ratio of 1: 1: 1; even more, around 42% of triads in Group A were missing either an A-, B-, or D-copy, a higher frequency than the 13.2% expected for all wheat proteins in the genome (Table 3). Group C, subclade C1, showed the most conserved 'clean' homoeologous triads (56.3%) such that there were rarely any singleton/orphan or 'nc' *TaFMOs*, and each *TaFMO* triad had corresponding orthologues from other grass species (Supplementary Figure S4); the high evolutionary conservation of these *TaFMO* triads is perhaps due to functional constraints influencing gene retention. In contrast, *TaFMOs* in subclade C2 (along with barley *FMO*s) appear to have large, uneven homeolog expansions via tandem duplications and intra- or interchromosomal dispersion of genes (Supplementary Figure S4).

In Group B, 36.4% of *TaFMOs* belong to even triads which more closely resemble the anticipated percentage (35.8%) of all predicted wheat proteins belonging to even homoeologous triads (Table 3) (Ramírez-González et al., 2018). Group B appears to have many instances of sub-genome homeolog expansion and uneven tandem duplications (Table 2). Subclade B1 appears to contain three pairs of *TaFMO* WGD homeologs that underwent multiple duplications, with more *HvFMO* orthologues present than *OsjFMO* and *TuFMO*, (Supplementary Figure S3), while subclade B2 shows *FMO* expansions for all grass species surveyed, but none for *Arabidopsis* (Supplementary Figure S3).

Such divergent patterns of gene retention and expansion among homoeologous triads between the three major groups of *TaFMOs* might implicate differing biological roles (Birchler and Yang, 2022). make a point that genes involved in defense mechanisms are more likely to diverge after duplication events; the retention of the active sites for some of the highly duplicated Group B triads could infer a role in defense-related functions.

TABLE 3 *TaFMO* Homeolog (triad) analysis.

Homoeolog ratios (A: B: D)	All wheat genes (2018)[§]	*TaFMO* Group A	*TaFMO* Group B	*TaFMO* Group C
1: 1: 1	35.80%	8.20%	36.36%	56.25%
n: 1: 1	5.70%	16.70%	45.44%	6.25%
1: n: 1				
1: 1: n[†]				
1: 1: 0	13.2%	41.70%	9.10%	12.50%
1: 0: 1				
0: 1: 1				
Orphans/ singletons[$]	37.10%	16.70%	--	6.25%
Other[¥]	8.00%	16.70%	9.10%	12.50%
Not Categorized[‡]	--	--	--	6.25%

[-] data not available.
[†] denotes n>1, where n represents either the A, B, or D subgenome copy duplicated as 2 or more copies.
[$] denotes orphaned/single TaFMO which were not found in synteny with any known triads.
[¥] denotes TaFMO which exhibited any A, B,and/or D subgenome duplication ratios not mentioned above.
[‡] unable to consolidate exact relation in synteny and phylogenetic analyses presented in this study.
[$] reported % of genes in wheat falling into each category by IWGSC 2018.

3.4 Variations in canonical motifs delineate the FMOs in wheat and related grasses

We detected fifteen of the most conserved protein motifs in FMOs across *Arabidopsis* and the grasses rice (*Osj*), barley (*Hv*), red einkorn (*Tu*) and wheat (Supplementary Figure S5). FMOs in plants are reported to contain three crucial protein motifs essential for 'canonical' FMO activity; these are the FAD-binding motif (GxGxxG), the NAD(P)H-binding motif (GxGxxG), and the FMO-identifying motif [FxGxxxHxxxY/F; (Eswaramoorthy et al., 2006; Hansen et al., 2007; Huijbers et al., 2014)]. While the FAD- and NAD(P)H-binding sites are active sites surrounding the enzyme pocket where hydroxylation takes place, the FMO-identifying motif is considered a linker region between the two active sites (Malito et al., 2004). The last and less widely talked about motif is the 'F/LATGY' motif, more recently referred to in some studies as the 'ATG-containing' or 'TGY' motif (Yoshimoto and Saito, 2015; Gaba et al., 2023); this motif is thought to be a crucial

TABLE 4 Transposable element status for *TaFMO* in Group A, B, and C.

FMOs in *T. aestivum* cv. Chinese Spring (RefSeqv2.1)	TE insertion inside	TE flanking (5' UTR, 3' UTR, both)
Total *TaFMO* (170)	44.7%	90.0%
–		
Group A TaFMO	60.0%	100.0%
Group B TaFMO	56.1%	91.2%
Group C TaFMO	27.0%	85.1%

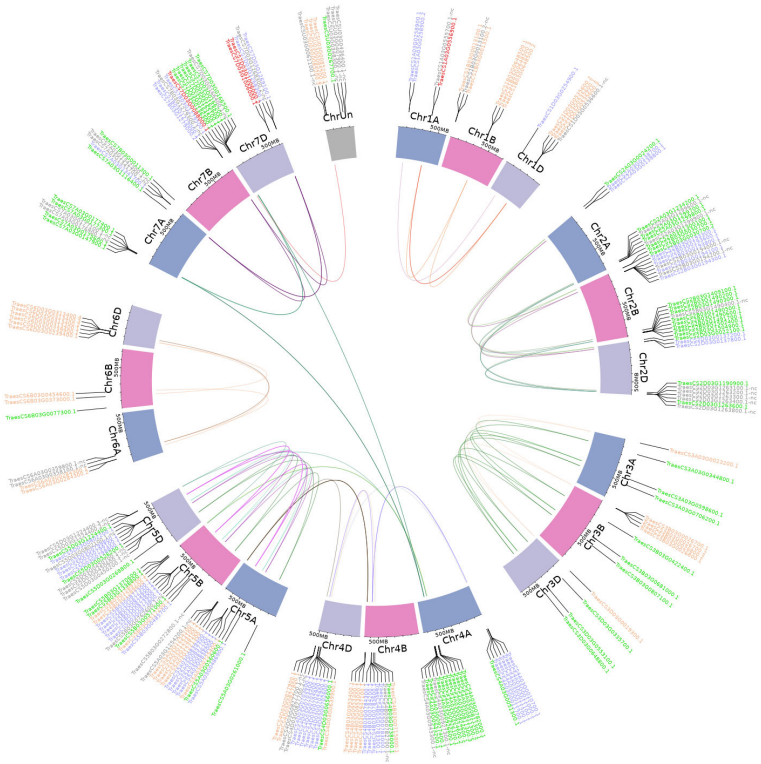

FIGURE 3
Genomic distribution of *TaFMO* groups A, B, and C candidates presented on a Circos plot (shinyCircos). Colors of gene labels correspond to the Group A (orange), B (blue) and C (green) partitions of *TaFMO* candidates. Red-labelled genes are orphaned/singleton *TaFMOs*, and grey-labelled genes are 'nc' *TaFMOs*. Cytobands exhibit chromosome tracks for chromosomes 1-7 (and unmapped chromosome, ChrUn) for each sub-genome A, B, and D in wheat. Links inside the circos plot are representative of whole-genome-duplication homeologs (syntenic triads) of wheat *TaFMO* genes delineated through a genome-wide synteny analysis; links are discretely colored in correspondence to annotated subclades for each of the *TaFMO* candidates, seen in Supplementary Figures S2-4, S2 notes.

factor governing *N*-hydroxylation (Stehr et al., 1998; Fennema et al., 2016).

The FAD-binding motif at the N-terminus is very well conserved with regards to three glycine residues across all groups (Figures 4A, B). However, the residues surrounding this motif for Group A and subclade B2 from Group B is recorded to be distinct from that in subclade B1 and Group C (Figures 4A, B; Supplementary Figures S2-4); the FAD-binding site variant 1 (for Group A and B2) and the other variant are highlighted in orange in Figure 4A, B. An extra copy of the FAD-binding variant 1 also exists between the NAD(P)H-binding site and the ATG-motif in most of the examined grass species (*Hv, Tu, Ta*) in subclade C2, but not for rice. This may indicate a novel function for FMOs specific to Triticeae. The NAD(P)H-binding motif across all FMOs (Supplementary Figure S5) is well-conserved for the first glycine residue, but not for the other two glycine residues (Gxgxxg; Figure 4A). The FMO-identifying motif for FMOs in Group A has the first residue swapped from the canonical F (Phenylalanine) for W (Tryptophan), which is the case for most of the plant species examined (Figure 4A). Additionally, the ATG-containing motif for Group A FMOs across all flowering plants surveyed are highly conserved, represented as HCTGY or YCTGY. The differences of the Group A ATG-motif and FMO-identifying motifs relative to Groups B and C may allude to specificity for *S*-oxygenation of compounds and specialized metabolites yet uncharacterized in cereals, where Group A FMOs from *A. thaliana* (FMO-GSOX enzymes) are well-characterized for their *S*-oxygenation activity during synthesis of specialized metabolites (Hansen et al., 2007). The ATG-containing motif is most varied for Group B FMOs, where in addition to the canonical '(F/L)ATGY' residues reported by (Schlaich, 2007), other variations are present (LATGF, FLATGF, FATGY, LATGY, FGTGF) in the B2 expanded subclade comprising other grass species (*Tu, Hv, Osj*). By contrast, Group C FMOs mostly present with 'LATGY' motifs (and some 'MATGY' motifs in barley and wheat) in subclade C1 and 'FATGY' motifs in subclade C2 (Figure 4A).

Beyond the documented protein motifs discussed above, one novel motif is reported for each Group A and Group C FMOs (referred to here as motif-A1 and motif-C1, respectively; see Supplementary Figure S5 for these and other motifs referred to in this section). Meanwhile, Group B FMOs have four clade-specific motifs (motif-B1-4) (Figure 4). Groups A, B, and C FMOs all share one novel motif each with each other (motif-AB1, motif-AC1, motif-BC1). Additionally, there is a novel motif common to almost all FMOs located at the N-terminus following the FAD-binding site for most FMOs, reported here as motif-ABC1 (Figure 4A). A look at predicted protein models highlights that many of these novel motifs may present as-yet-unclassified linker

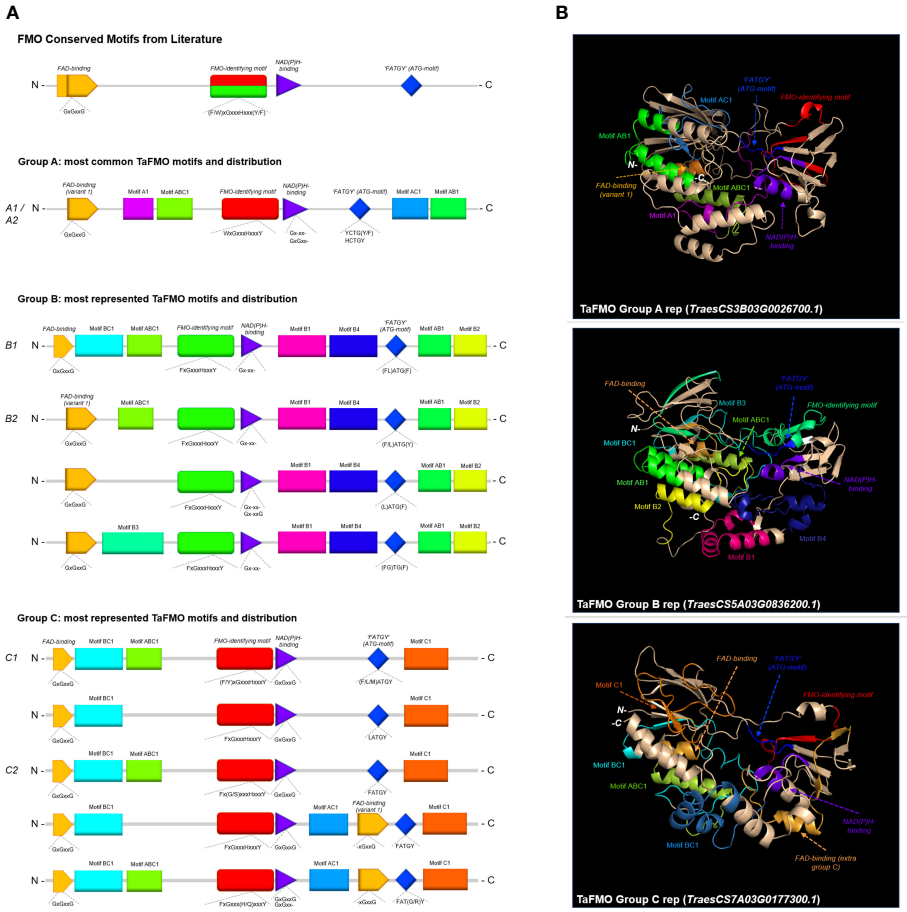

FIGURE 4
(A) Consensus MEME motifs for conserved and unique motifs across Groups A, B, and C TaFMO proteins. **(B)** Predicted 3D protein structures for Groups A, B, and C TaFMO with highlighted motifs.

regions contributing to the integrity of the enzyme, or motifs that govern substrate specificity and binding affinity (Figure 4B). We hypothesize that differences in tertiary protein structures, including these clade-specific motifs, likely play a crucial role in substrate specificity (Li et al., 2008; Zhu et al., 2019). While no plant FMOs have been crystalized to date, the use of 3D protein homology modelling and ligand-docking simulations—in corroboration with functional analyses—may shed some light on which compounds TaFMO, and other cereal FMOs, may be acting upon.

3.5 Possible roles of group A and C TaFMO: from pathogen defense to grain development

Group A *FMO*s contain all the *Arabidopsis FMO-GSOX* (glucosinolate oxidase) genes. These FMOs have been experimentally validated to participate in glucosinolate (GSL) biosynthesis by catalyzing the *S*-hydroxylation of methylthioalkyls to methylsulfinylalkyls, where GSLs are a class of specialized sulphur-containing metabolites involved in plant-herbivory defenses (Hansen et al., 2007; Li et al., 2011; Kong et al., 2016; Cang et al., 2018; Schall et al., 2020). GSLs are predominantly found in the mustard seed family (Brassicaceae), although there is evidence that 500 neighboring eudicot species outside this family may also contain one or more of the 120 documented GSLs (Flamini, 2012). The possible metabolites that these Group A FMOs help modify in cereals are not well-understood, as cereals are not reported to produce GSLs (Hansen et al., 2007; Thodberg and Jakobsen Neilson, 2020). More recently, other *A. thaliana* FMOs have been documented to synthesize trimethylamine *N*-oxide (TMAO) (Fennema et al., 2016), the levels of which are increased in plants under low temperatures, drought, and high salt stress conditions (Catalá et al., 2021). Group A *FMO*s segregate into two major subclades, A1 and A2 (Figures 2, Supplementary Figure S2). While little is known for Group A *FMO*s in barley and red einkorn, it is reported that five rice *FMO*s from subclade A1 (*Os01t0368000-nc, Os02t0580600-nc, Os07t0111700, Os07t0111900, Os07t0112000*) are co-expressed with *WRKY13* (a transcription factor involved in pathogen defense) upon attack by rice sheath-infecting fungi (John Lilly and Subramanian, 2019). For *TaFMO*s in subclade A1, the literature supports involvement in root drought tolerance, tiller growth, and nutrient accumulation in the grain (Table 2; Supplementary Figure S6). The rice *FMO*

Os10t0553800 in subclade A2 may play an important role in rice germination and seedling establishment during floods, via epigenetic methylation responses to anaerobic conditions (Castano-Duque et al., 2021). By contrast, several *TaFMOs* in subclade A2 are implicated in disease resistance against both biotrophic (Navathe et al., 2022) and necrotrophic pathogens (Nussbaumer et al., 2015), in addition to root drought tolerance (Supplementary Figure S6). The amino oxidase (AOX) protein domain which is seen in almost all FMOs in Group A at the N-terminus but rarely for Group B (and which is missing from Group C), is larger in subclade A2 AtFMOs (~150 amino acid residues), but not for wheat (~60 residues) or other plant FMOs (Figure 2). The AOX domain in Group A TaFMOs appears to encompass the motif-A1 mentioned previously unique to Group A and may participate in substrate binding specificity for novel compounds in wheat.

Group C contains the "*YUCCA*" (*YUC*) genes that are known to participate in auxin (idole-3-acetic acid, IAA) biosynthesis (Kendrew, 2001; Cao et al., 2019), where auxin is involved in many plant development processes (Schlaich, 2007; Chandler, 2015). We identified 74 *TaFMOs* in Group C, which can be split into two main subclades, C1 and C2. Several *TaFMOs* in subclade C1 are implicated in the response to drought stress (Table 2; Supplementary Figure S7), found to be upregulated during root drought treatment (Grzesiak et al., 2019), or associated with an increased reactive oxygen species (ROS, H_2O_2) burst in response to root drought conditions (Kamruzzaman et al., 2022). In subclade C2, several *TaFMOs* are implicated in plant development, including in grain (Mangini et al., 2021) and seed development (Li et al., 2014), and tiller number increase (Yu et al., 2021). To date, only three homoeologous genes involved in seed development have been functionally characterized via gene cloning (Li et al., 2014). A catalogue of 63 '*TaYUC*' gene candidates involved in auxin biosynthesis by Yang et al. (2021) included several *TaFMO* genes outside Group C (dispersed throughout subclade B2; Supplementary Table S4), hinting towards a flexibility in *TaFMO* involvement in auxin biosynthesis-regulated plant development. In the absence of a full gene family survey and experimental characterization, adopting a more wheat-specific nomenclature for the *FMO* gene family via the guidelines put forward by the Wheat Initiative community (Boden et al., 2023), may minimize confusion on gene names in wheat to streamline future research efforts.

3.6 Group B TaFMOs: major players in broad-spectrum disease resistance

Group B *FMO*s can be split into two distinct subclades, B1 and B2 (Figure 2). This group contains the *Arabidopsis AtFMO1* and *AtFMO2* genes. AtFMO1 hydroxylates the N atom of an L-lysine catabolic product to form *N*-hydroxylated pipecolic acid (NHP), crucial for establishing systemic acquired resistance (SAR) to combat microbial pathogen invasions (Conrath, 2006; Mishina and Zeier, 2006; Chen et al., 2018; Hartmann et al., 2018), and a lack of NHP (due to defects in its biosynthesis) results in immunocompromised *Arabidopsis* plants. Various studies have recently contributed to better understanding the mechanism of NHP-mediated SAR regulation in other plants, including cereal crops, by searching for functional orthologs to *AtFMO1* and their possible involvement in disease resistance (Holmes et al., 2019; Lenk et al., 2019; Schnake et al., 2020; Vlot et al., 2021; Zhang et al., 2021).

In subclade B1, *AtFMO1* and *AtFMO2*, the only Group B *FMOs* in *Arabidopsis*, form a clade with 18 *TaFMOs*, where only three candidates are 'nc' (Table 2, Figure 4B). All FMOs from subclade B1 possess the most minimal number of known protein domains via SMART analysis, whereas multiple protein domains are present for TaFMO from all other clades (Figure 2). Of note, AtFMO1 harbors an additional K-oxygenase domain (IPR025700) in the first half of its protein sequence, which is not seen in any of the B1 TaFMOs or AtFMO2 but is present in most B2 TaFMOs and TaFMOs in Groups A and C. The K-oxygenase domain is involved in siderophore biosynthesis, and in ornithine and lysine hydroxylation (Visca et al., 1994; Krithika et al., 2006); therefore, presence of this K-oxygenase may play a critical role in hydroxylation of L-lysine and/or L-ornithine derived compounds.

While subclade B1 *TaFMOs* show little to no transcriptional activity in the conditions surveyed, certain subclade B2 *TaFMO*s exhibit higher transcriptional activity (Figures 2, 5 – III/IV). The *TaFMO TraesCS5D03G0799800.1* in subclade B2 (B2β-3b) was detected as the most transcriptionally upregulated "FMO1-like" *TaFMO* in response to treatment of wheat coleoptiles with NHP (Zhang et al., 2021). Two homoeologous triads in B2α-2 (Table 2) show transcriptional upregulation in root, stem, and leaf tissues (Figure 2), and peptide abundance of these triads was also detected in a wide variety of wheat tissues (Figure 5 – II). These *TaFMOs* in B2α-2 undergo transcriptional activation in wheat seedlings during infection by the fungal pathogens *Zymoseptoria tritici* (*Zt*) (Yang et al., 2013; Rudd et al., 2015) and *Puccinia striiformis* f.sp. *tritici* (*Pst*) (Cantu et al., 2013; Dobon et al., 2016), but have very little to no transcriptional activation during older developmental stages of wheat, such as seen in controls during infections by *Fusarium graminearum* (*Fg*) in the wheat grain head (Schweiger et al., 2016) and *Magnaporthe oryza* (*Mo*) at the grain-filling stage (Islam et al., 2016) (Figure 5 - III).

One of the B2α-2 homoeologous triads (*TraesCS5A03G0836200.1, TraesCS5B03G0873900.1, TraesCS5D03G0799100.1*) shows greater upregulation of transcription after *Pst* infection at one day post-infection (dpi), which is sustained through 11 dpi; *TraesCS5A03G0836200.1* is also reported by (Vikas et al., 2022) in a genome-wide association study (GWAS) to be likely involved in seedling resistance to the biotrophic fungal pathogen *Puccinia triticina* (*Pt*), the wheat leaf rust pathogen closely related to *Pst*. Another *TaFMO* in sub-clade B2β-4c(2), *TraesCS7B03G1279500.1*, might be involved in *Puccinia graminis* f.sp *tritici* (*Pgt*, stem rust) resistance (Sahu et al., 2021). In a QTL analysis by (Matros et al., 2017), the two triads in subclade B2α-2 were also detected as significantly enriched in SNPs associated with ornithine metabolism in wheat. Ornithine is an amino acid bearing great resemblance to lysine and has functional significance in plant abiotic stress tolerance (Kalamaki et al., 2009) through its role in osmoregulation during drought and salinity stress (Roosens et al., 1998; Xue et al., 2009). These two triads are among the only Group B *TaFMOs* to be transcriptionally responsive in the abiotic conditions presented, downregulated during

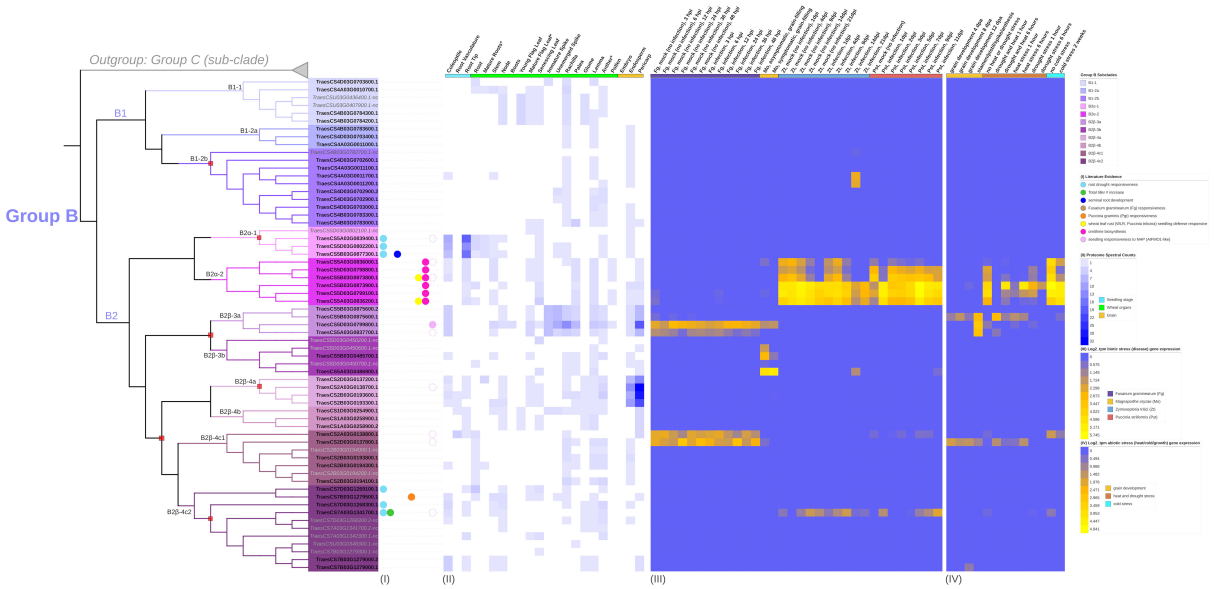

FIGURE 5
Transcription of group B *TaFMOs* under various conditions explored from literature data. (Columns I) reports of previous evidence of transcript detection or cloning under various conditions described in the legend. (Columns II) Protein expression (spectral peptide counts) for each candidate in various tissues from https://wheatproteome.org/ (Duncan et al., 2017). (Columns III) Heatmap of *TaFMO* transcripts in response to four types of biotic stresses; response to *Fusarium graminearum* infection(*Fg*) (Schweiger et al., 2016), mock inoculation versus pathogen infection in a time-course of 3, 6, 12, 24, 36, and 48 hours post infection (hpi); *Magnaporthe oryza* (*Mo*) (Islam et al., 2016), asymptomatic (control) versus symptomatic (infection) conditions at grain-filling stage; *Zymoseptoria tritici* (*Zt*) (Yang et al., 2013; Rudd et al., 2015), mock inoculation versus pathogen infection in a time-course of 1, 4, 9, 14, 21 days post infection (dpi); *Puccinia striiformis* f.sp. *tritici* (*Pst*) (Cantu et al., 2013; Dobon et al., 2016), uninfected control versus pathogen infection in a time-course of 1, 2, 3, 5, 7, 9, 11 dpi. (Columns IV) Heatmap of *TaFMO* transcript response to grain development over a time-course (4, 8 12 days post anthesis) (Li et al., 2013; Yang et al., 2015), heat and drought stress (1 and 6 hours) (Liu et al., 2015), and cold stress (control versus 2-week cold stress) (Li et al., 2015). Heatmap data is displayed as Log2 transcripts per million (tpm), with blue being 0 and higher-fold expression approaching bright yellow (see legends).

drought stress, heat stress, and combined drought + heat stress at one hour, but bounce back to nearly control levels after six hours of treatment for certain splice variants (Figure 5 – IV) (Liu et al., 2015). Transcripts of the *TaFMO* triad in B2α-1 (except for the 'nc' 5D homeolog) have been detected in wheat roots (Figure 2, Table 2) (Grzesiak et al., 2019). reported that genes of this triad were upregulated in response to water deprivation in wheat root tissues, though no upregulation of transcription in leaf tissues was detected in the drought study by Liu et al. (2015) (Figure 5 – IV), highlighting a need for careful interpretation of tissue-specific expression patterns of *TaFMOs*. Furthermore, a GWAS analysis indicates that the B-copy gene of this triad, *TraesCS5B03G0877300.1*, influences root-growth and biomass yield-related traits (Zhao et al., 2023). Trends for other candidates of interest are found in Appendix S7.

In summary, several lines of evidence hint at roles in responsiveness to various microbial diseases for several *TaFMOs* in subclade B2. Additionally, certain subclade B2 *TaFMOs* may operate during plant development (tiller increase) and drought, heat, and salinity tolerance. Thodberg et al. (2020) showed that a novel Group B FMO in fern (FOS1) participates in both the *N*-hydroxylation of a novel class of metabolites not previously reported in vascular plants and in the biosynthesis of cyanogenic glycoside. Likewise, the exploration and characterization of these B2 *TaFMOs* may identify novel functions and metabolites towards plant development, biotic, and abiotic stressors.

3.7 TaFMO UTRs are populated with elements involved in complex regulation

Untranslated regions in transcripts (UTRs) have been reported in plants as important regulatory regions often harboring important *cis*-acting regulatory elements (CAREs) that influence gene expression, modulate translational efficiency, and increase the coding capacity of genes that have different splice variations (Mignone et al., 2002; Srivastava et al., 2018). We found a wide variety of CAREs in the promoter regions 1.5 kb upstream of the start codon of *TaFMO* genes (Figures 6; Supplementary Figures S8, S9). The presence and sizes of 5'- and 3'-UTRs among *TaFMOs* varied; we observed that for all *TaFMOs*, the 3'-UTRs were longer than the 5'-UTRs, when UTRs were present (Figures 7; Supplementary Figures S10, S11). Srivastava et al. (2018) reported elongated UTRs (particularly 3'-UTRs) in rice compared to *Arabidopsis*. In wheat, 3'-UTRs have also been reported to have a critical involvement in mediating drought stress (Ma et al., 2023) and in establishing resistance against stripe rust (Zhang et al., 2019), possibly through regulating mRNA stability. Of note, all the tandemly duplicated wheat *TaFMOs* in subclade C2 lack any UTRs (Supplementary Figure S11) and show virtually no (or low) transcript responsiveness to the biotic and abiotic conditions explored (Supplementary Figure S7 – III, IV), with minimal presence of expressed peptides detected in various tissue types.

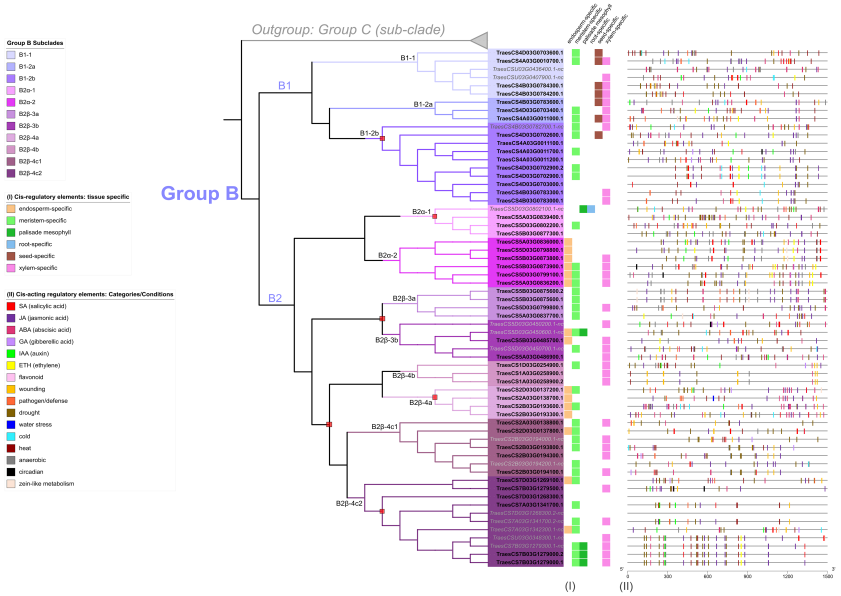

FIGURE 6
Plant *cis*-acting regulatory elements (CARE) detected in a 1.5 kb region upstream of start codons for all *TaFMO* in Group B X-axis denote the number of base pairs away from the start codon, where 5′ is 1,500 bp upstream ATG start codon (3′ and 0 bp is right before the ATG start codon). Polytomy regions are denoted by a red box. Presence of regulatory elements specific to different tissues are described in (I). Other responsive promoter elements are denoted in the figure legend and displayed as rectangles of corresponding color to the condition in (II).

Focusing on the Group B *TaFMO*s, analysis of the CAREs revealed involvement in responsiveness to major phytohormones and conditions (Figure 6; Appendix S5). Jasmonic acid (JA)-responsive CAREs were present in all *TaFMO* promoters at one or multiple sites; JA is a phytohormone known for involvement in many plant processes ranging broadly from photosynthesis to heat stress-responsiveness (Per et al., 2018), but most widely documented for defense against necrotrophic pathogens (Qi et al., 2016) and induced systemic resistance (Heil, 2002). In wheat, JA-signaling has also been implicated in seedling salt-stress tolerance (Qiu et al., 2014). Other notable phytohormone-responsive CAREs in Group B are for salicylic acid (SA), gibberellic acid (GA) and ethylene (ETH) (Supplementary Tables S3, 4, Figure 6). SA is a major phytohormone involved in SAR and pathogen defense signaling pathways (Dey et al., 2014; Ding et al., 2018). SA-responsive CAREs were found in higher abundance and closer to the start codons of the triads from B2α-2 (Figure 6, Supplementary Table S4), whose genes were more transcriptionally active in *Zt*- and *Pst*-infected wheat (Figure 5 – III); this may indicate that number and location of these CAREs influence which *TaFMOs* are activated under pathogen stress. GA is a phytohormone that was documented in wheat for its involvement in enhancing disease resistance against *F. graminearum* infection, by modulating both primary and specialized metabolism during early plant defense signaling (Buhrow et al., 2021); GA-responsive CAREs are found predominantly in subclade B2, further supporting that *TaFMOs* in this subclade are likely involved in microbial disease resistance. Auxin (IAA)-responsive CAREs are found to be abundant among many Group B *TaFMOs* (Supplementary Table S4), challenging the idea of Group C *TaFMOs*—the '*YUCCA*' *FMO* clade—being largely responsible for auxin biosynthesis and growth regulation in plants for underreported crop species (Kendrew, 2001).

3.8 Transposable elements, gene structure diversity, and differential TaFMO expression

We explored transposable element (TE) distribution in or near the identified *TaFMO* genes and affecting intron-exon structure to find support for relationships among *TaFMO* family members (Figure 7, Supplementary Figures S10, 11; Appendix S6). Focusing again on the Group B *TaFMOs*, we observed much variation in the number and spatial distribution of introns and exons; high similarity of gene structures was found among certain syntenic triads highlighting distinct *TaFMO* subfamilies that possibly remain conserved for functional importance. In contrast, extensive intron-exon shuffling following gene duplication events (Kolkman and Stemmer, 2001; França et al., 2012) may indicate lower selective pressure and neofunctionalization, such as in the case for subclades B2β-4c1 and B2β-4c2 (Figure 7).

Nearly all *TaFMO*s (90%) are flanked by TEs within a 2 kb region upstream and/or downstream of the start or stop codons (Figure 7, Table 4) in accordance with a report of TEs representing over 80% of the wheat genome (Choulet et al., 2014; Bariah et al., 2020). 44.7% of all *TaFMO* genes show disruption by TE insertion, mostly occurring inside introns, inside 5'- or 3'-UTRs, or, very rarely, inside exons (Figure 7). TE insertions are present in 56.1% of Group B *TaFMO*, with the largest TE interruption in *TraesCS2B03G0193800* increasing its total gene length to upwards of 29 kb (Figure 7). Most TE disruptions in subclade B2 occur in the B- and D-copy homeologs

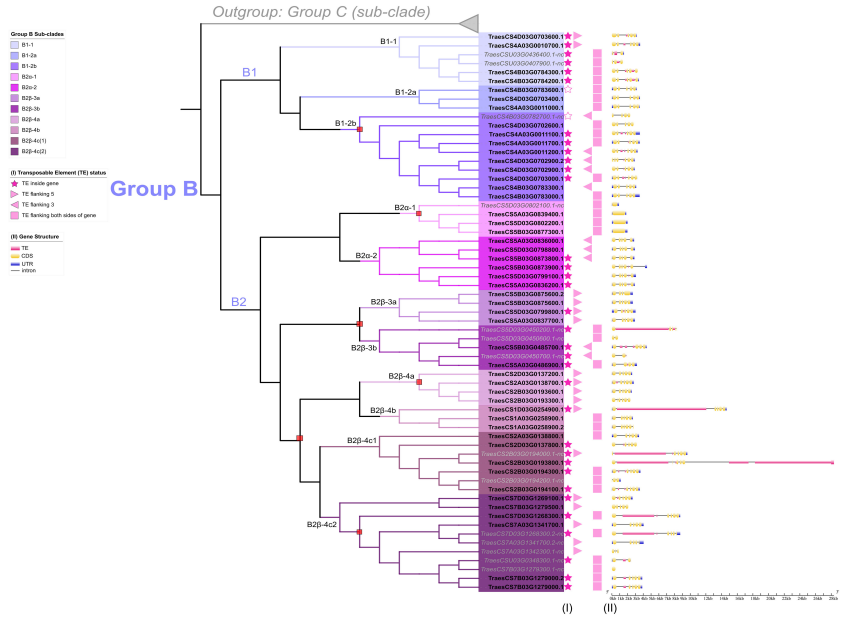

FIGURE 7
Graphical display of the gene structure and transposable element analysis for *TaFMOs* in Group B Polytomies are denoted by a red box at respective nodes on the ML tree. Status of TE distribution is described in (I) for filled star: TE insertion inside gene; unfilled star: non-coding region of TE spanning entire gene; filled triangle: TE flanking either 5′ or 3′ UTR of gene; and filled square: TE flanking both sides of the gene. A 2 kb region upstream of the start codon and downstream of the stop codon were scanned for flanking TEs. (II) The gene structure is displayed for each *TaFMO*, with graphical depiction of TE insertion, if present. The X-axis scale describes the size in kb of nucleotides for each gene region. In Group B, exon numbers vary from three to five (B1), one (B2α-1), and one to five (all rest of sub-clade B2).

and appear to be correlated with differential expression patterns among homoeologous triads. Varying locations of TE insertions in the highly tandemly duplicated B-copy *TaFMOs* in B2β-4c(1) correlate with no transcriptional expression compared to the A- and D-copies, and only an A-copy *TaFMO* in B2β-4c(2) lacking TE insertions was transcriptionally active (Figure 5 – III, IV; Figure 7). In contrast, one of the triads in B2α-2 (*TraesCS5A03G0836200, TraesCS5B03G0873900, TraesCS5D03G0799100*) shares the same TE insertion in its three members, which are all more transcriptionally active than gene members in the other B2α-2 triad lacking this TE insertion, particularly upregulated towards *Pst* infection and cold stress responses (Figure 5 – III, IV; Figure 7).

Yang et al. (2021) reported on the gene structure of a candidate '*YUCCA*' *FMO* in wheat, *TaYUCCA5-D* (*TraesCS1D03G0254900.1*, Group B), containing a first intron size of approximately 13 kb. We now know this is due to a TE insertion (Figure 7), underscoring a need for expanding on factors driving gene structure diversity in large gene-family analyses. We see that TE insertions in the intronic and 3'-UTR regions may play a role in influencing gene expression of triads on a sub-genome level, possibly leading to eventual neofunctionalization of *FMO* family members. Several studies indicate that TEs are important drivers in polyploid plant evolution (Vicient and Casacuberta, 2017; Gill et al., 2021), such as in wheat where distinct TE families are correlated with up- or down-regulation of genes in their vicinity (Bariah et al., 2023). Thus, exploring classes of TE elements that lie in or around *TaFMOs* could aid in predicting gene expression regulation in the different wheat sub-genomes.

4 Concluding remarks

We present here a comprehensive phylogenetic analysis of the *FMO* superfamily in wheat and integrate various publicly available transcriptomic and proteomic data to shed light on the breadth of expansion for this superfamily in wheat and predict potential roles for the members of this family for hypothesis generation and further functional studies. We show that *TaFMOs* segregate into three distinct groups, and that unique domain architectures and protein motifs may indicate ligand-binding specificities among sub-groups of *TaFMOs*. We corroborate the expression data from existing literature of certain candidate *TaFMOs* with their possible biological functions as discussed in various studies. This study provides a solid foundation for the further exploration and functional characterization of the *FMO* gene family in common wheat.

Data availability statement

The original contributions presented in the study are included in the article/Supplementary Material. Further inquiries can be directed to the corresponding author.

Author contributions

SS: Data curation, Formal analysis, Investigation, Software, Visualization, Writing – original draft. GB: Conceptualization, Funding acquisition, Supervision, Writing – review & editing.

Funding

The author(s) declare that financial support was received for the research, authorship, and/or publication of this article. Funding was provided by the Natural Sciences and Engineering Research Council of Canada, CREATE grant (509257-2018) and Natural Sciences and Engineering Research Council of Canada, Canada Graduate Scholarship – Doctoral award (CGSD-579396-2023).

Acknowledgments

We thank our funding support by the Natural Sciences and Engineering Research Council of Canada (NSERC) CREATE program, as well as the NSERC CGS-D program. The authors are indebted to Dr. Sean Graham for help reviewing the phylogenetic analyses, manuscript editing and valuable discussions. Additionally, we thank Dr. Matthias Kretschmer for his constructive feedback on the original manuscript.

Conflict of interest

The authors declare that the research was conducted in the absence of any commercial or financial relationships that could be construed as a potential conflict of interest.

Publisher's note

All claims expressed in this article are solely those of the authors and do not necessarily represent those of their affiliated organizations, or those of the publisher, the editors and the reviewers. Any product that may be evaluated in this article, or claim that may be made by its manufacturer, is not guaranteed or endorsed by the publisher.

Supplementary material

The Supplementary Material for this article can be found online at: https://www.frontiersin.org/articles/10.3389/fpls.2024.1369299/full#supplementary-material

References

Bailey, T. L., Johnson, J., Grant, C. E., and Noble, W. S. (2015). The MEME suite. *Nucleic Acids Res.* 43, W39–W49. doi: 10.1093/nar/gkv416

Bariah, I., Gribun, L., and Kashkush, K. (2023). Transposable elements are associated with genome-specific gene expression in bread wheat. *Front. Plant Sci.* 13. doi: 10.3389/fpls.2022.1072232

Bariah, I., Keidar-Friedman, D., and Kashkush, K. (2020). Where the wild things are: transposable elements as drivers of structural and functional variations in the wheat genome. *Front. Plant Sci.* 11. doi: 10.3389/fpls.2020.585515

Birchler, J. A., and Yang, H. (2022). The multiple fates of gene duplications: Deletion, hypofunctionalization, subfunctionalization, neofunctionalization, dosage balance constraints, and neutral variation. *Plant Cell* 34, 2466–2474. doi: 10.1093/plcell/koac076

Boden, S. A., McIntosh, R. A., Uauy, C., Krattinger, S. G., Dubcovsky, J., Rogers, W. J., et al. (2023). Updated guidelines for gene nomenclature in wheat. *Theor. Appl. Genet.* 136, 72. doi: 10.1007/s00122-023-04253-w

Buhrow, L. M., Liu, Z., Cram, D., Sharma, T., Foroud, N. A., Pan, Y., et al. (2021). Wheat transcriptome profiling reveals abscisic and gibberellic acid treatments regulate early-stage phytohormone defense signaling, cell wall fortification, and metabolic switches following *Fusarium graminearum*-challenge. *BMC Genomics* 22, 798. doi: 10.1186/s12864-021-08069-0

Cang, W., Sheng, Y.-X., Evivie, E. R., Kong, W.-W., and Li, J. (2018). Lineage-specific evolution of flavin-containing monooxygenases involved in aliphatic glucosinolate side-chain modification: Evolution of flavin-containing monooxygenases. *J. Systematics Evol.* 56, 92–104. doi: 10.1111/jse.12289

Cantu, D., Segovia, V., MacLean, D., Bayles, R., Chen, X., Kamoun, S., et al. (2013). Genome analyses of the wheat yellow (stripe) rust pathogen *Puccinia striiformis* f. Sp. *Tritici* reveal polymorphic and haustorial expressed secreted proteins as candidate effectors. *BMC Genomics* 14, 270. doi: 10.1186/1471-2164-14-270

Cao, X., Yang, H., Shang, C., Ma, S., Liu, L., and Cheng, J. (2019). The roles of Auxin biosynthesis *YUCCA* gene family in plants. *Int. J. Mol. Sci.* 20, 6343. doi: 10.3390/ijms20246343

Castano-Duque, L., Ghosal, S., Quilloy, F. A., Mitchell-Olds, T., and Dixit, S. (2021). An epigenetic pathway in rice connects genetic variation to anaerobic germination and seedling establishment. *Plant Physiol.* 186, 1042–1059. doi: 10.1093/plphys/kiab100

Catalá, R., López-Cobollo, R., Berbís, M.Á., Jiménez-Barbero, J., and Salinas, J. (2021). Trimethylamine *N* -oxide is a new plant molecule that promotes abiotic stress tolerance. *Sci. Adv.* 7, eabd9296. doi: 10.1126/sciadv.abd9296

Chandler, J. W. (2015). "Auxin biosynthesis," in *Amino acids in higher plants*, *1st ed.* Ed. J. P. F. D'Mello (CAB International), 340–361. doi: 10.1079/9781780642635.0340

Chen, K., Durand, D., and Farach-Colton, M. (2000). NOTUNG: A program for dating gene duplications and optimizing gene family trees. *J. Comput. Biol.* 7, 429–447. doi: 10.1089/106652700750050871

Chen, Y.-C., Holmes, E. C., Rajniak, J., Kim, J.-G., Tang, S., Fischer, C. R., et al. (2018). *N* -hydroxy-pipecolic acid is a mobile metabolite that induces systemic disease resistance in *Arabidopsis*. *Proc. Natl. Acad. Sci.* 115 (21), E4920–E4929. doi: 10.1073/pnas.1805291115

Chen, C., Wu, Y., and Xia, R. (2022). A painless way to customize Circos plot: From data preparation to visualization using TBtools. *iMeta* 1, e35. doi: 10.1002/imt2.35

Choulet, F., Alberti, A., Theil, S., Glover, N., Barbe, V., Daron, J., et al. (2014). Structural and functional partitioning of bread wheat chromosome 3B. *Science* 345, 1249721. doi: 10.1126/science.1249721

Conrath, U. (2006). Systemic acquired resistance. *Plant Signaling Behav.* 1 (4), 179–84. doi: 10.4161/psb.1.4.3221

Curtis, T., and Halford, N. G. (2014). Food security: The challenge of increasing wheat yield and the importance of not compromising food safety. *Ann. Appl. Biol.* 164, 354–372. doi: 10.1111/aab.12108

Czarnocka, W., Fichman, Y., Bernacki, M., Różańska, E., Sańko-Sawczenko, I., Mittler, R., et al. (2020). FMO1 is involved in excess light stress-induced signal transduction and cell death signaling. *Cells* 9, 2163. doi: 10.3390/cells9102163

Dey, S., Wenig, M., Langen, G., Sharma, S., Kugler, K. G., Knappe, C., et al. (2014). Bacteria-triggered systemic immunity in barley is associated with WRKY and ETHYLENE RESPONSIVE FACTORs but not with salicylic acid. *Plant Physiol.* 166, 2133–2151. doi: 10.1104/pp.114.249276

Ding, Y., Sun, T., Ao, K., Peng, Y., Zhang, Y., Li, X., et al. (2018). Opposite roles of salicylic acid receptors NPR1 and NPR3/NPR4 in transcriptional regulation of plant immunity. *Cell* 173 (6), P1454–1467.E15. doi: 10.1016/j.cell.2018.03.044

Dobon, A., Bunting, D. C. E., Cabrera-Quio, L. E., Uauy, C., and Saunders, D. G. O. (2016). The host-pathogen interaction between wheat and yellow rust induces temporally coordinated waves of gene expression. *BMC Genomics* 17, 380. doi: 10.1186/s12864-016-2684-4

Duncan, O., Trösch, J., Fenske, R., Taylor, N. L., and Millar, A. H. (2017). Resource: Mapping the *Triticum aestivum* proteome. *Plant J.* 89, 601–616. doi: 10.1111/tpj.13402

Eswaramoorthy, S., Bonanno, J. B., Burley, S. K., and Swaminathan, S. (2006). Mechanism of action of a flavin-containing monooxygenase. *Proc. Natl. Acad. Sci.* 103, 9832–9837. doi: 10.1073/pnas.0602398103

Fennema, D., Phillips, I. R., and Shephard, E. A. (2016). Trimethylamine and Trimethylamine N-oxide, a Flavin-containing Monooxygenase 3 (FMO3)-mediated host-microbiome metabolic axis implicated in health and disease. *Drug Metab. Disposition* 44, 1839–1850. doi: 10.1124/dmd.116.070615

Felsenstein, J. (1985). Confidence limits on phylogenies: an approach using the bootstrap. *Evolution* 39 (4), 783–791. doi: 10.1111/j.1558-5646.1985.tb00420.x

Flamini, G. (2012). "Natural herbicides as a safer and more environmentally friendly approach to weed control: A review of the literature since 2000," in *Studies in Natural Products Chemistry*, vol. 38. (Elsevier), 353–396. doi: 10.1016/B978-0-444-59530-0.00013-7

França, G. S., Cancherini, D. V., and De Souza, S. J. (2012). Evolutionary history of exon shuffling. *Genetica* 140, 249–257. doi: 10.1007/s10709-012-9676-3

Gaba, Y., Bhowal, B., Pareek, A., and Singla-Pareek, S. L. (2023). Genomic survey of Flavin monooxygenases in wild and cultivated rice provides insight into evolution and functional diversities. *Int. J. Mol. Sci.* 24, 4190. doi: 10.3390/ijms24044190

Gill, R. A., Scossa, F., King, G. J., Golicz, A. A., Tong, C., Snowdon, R. J., et al. (2021). On the role of transposable elements in the regulation of gene expression and subgenomic interactions in crop genomes. *Crit. Rev. Plant Sci.* 40, 157–189. doi: 10.1080/07352689.2021.1920731

Grzesiak, M. T., Hordyńska, N., Maksymowicz, A., Grzesiak, S., and Szechyńska-Hebda, M. (2019). Variation among spring wheat (*Triticum aestivum* L.) genotypes in response to the drought stress. II—Root system structure. *Plants* 8, 584. doi: 10.3390/plants8120584

Hallgren, J., Tsirigos, K. D., Pedersen, M. D., Almagro Armenteros, J. J., Marcatili, P., Nielsen, H., et al. (2022). DeepTMHMM predicts alpha and beta transmembrane proteins using deep neural networks. *Bioinformatics*. doi: 10.1101/2022.04.08.487609. [Pre-print]

Hansen, B. G., Kliebenstein, D. J., and Halkier, B. A. (2007). Identification of a flavin-monooxygenase as the *S*-oxygenating enzyme in aliphatic glucosinolate biosynthesis in Arabidopsis: Identification of a flavin monooxygenase. *Plant J.* 50, 902–910. doi: 10.1111/j.1365-313X.2007.03101.x

Hartmann, M., Zeier, T., Bernsdorff, F., Reichel-Deland, V., Kim, D., Hohmann, M., et al. (2018). Flavin monooxygenase-generated *N*-hydroxypipecolic acid is a critical element of plant systemic immunity. *Cell* 173, 456–469.e16. doi: 10.1016/j.cell.2018.02.049

Heil, M. (2002). Induced systemic resistance (ISR) against pathogens in the context of induced plant defences. *Ann. Bot.* 89, 503–512. doi: 10.1093/aob/mcf076

Holmes, E. C., Chen, Y.-C., Sattely, E. S., and Mudgett, M. B. (2019). An engineered pathway for *N* -hydroxy-pipecolic acid synthesis enhances systemic acquired resistance in tomato. *Sci. Signaling* 12, eaay3066. doi: 10.1126/scisignal.aay3066

Hu, B., Jin, J., Guo, A.-Y., Zhang, H., Luo, J., and Gao, G. (2015). GSDS 2.0: An upgraded gene feature visualization server. *Bioinformatics* 31, 1296–1297. doi: 10.1093/bioinformatics/btu817

Huijbers, M. M. E., Montersino, S., Westphal, A. H., Tischler, D., and van Berkel, W. J. H. (2014). Flavin dependent monooxygenases. *Arch. Biochem. Biophysics* 544, 2–17. doi: 10.1016/j.abb.2013.12.005

International Wheat Genome Sequencing Consortium, Wicker, T., Gundlach, H., Spannagl, M., Uauy, C., Borrill, P., et al. (2018a). Impact of transposable elements on genome structure and evolution in bread wheat. *Genome Biol.* 19, 103. doi: 10.1186/s13059-018-1479-0

Islam, M. T., Croll, D., Gladieux, P., Soanes, D. M., Persoons, A., Bhattacharjee, P., et al. (2016). Emergence of wheat blast in Bangladesh was caused by a South American lineage of *Magnaporthe oryzae*. *BMC Biol.* 14, 84. doi: 10.1186/s12915-016-0309-7

Jermiin, L. S. (2017). *Homo version 1.3* (CSIRO). *Data Access Portal.* [Computer software]. Canberra, Australia. doi: 10.4225/08/5a56c7a9e4c2a

Jermiin, L. S., Catullo, R. A., and Holland, B. R. (2020). A new phylogenetic protocol: Dealing with model misspecification and confirmation bias in molecular phylogenetics. *NAR Genomics Bioinf.* 2, lqaa041. doi: 10.1093/nargab/lqaa041

John Lilly, J., and Subramanian, B. (2019). Gene network mediated by WRKY13 to regulate resistance against sheath infecting fungi in rice (*Oryza sativa* L.). *Plant Sci.* 280, 269–282. doi: 10.1016/j.plantsci.2018.12.017

Kalamaki, M. S., Merkouropoulos, G., and Kanellis, A. K. (2009). Can ornithine accumulation modulate abiotic stress tolerance in *Arabidopsis*? *Plant Signaling Behav.* 4, 1099–1101. doi: 10.4161/psb.4.11.9873

Kalyaanamoorthy, S., Minh, B. Q., Wong, T. K. F., von Haeseler, A., and Jermiin, L. S. (2017). ModelFinder: Fast model selection for accurate phylogenetic estimates. *Nat. Methods* 14, 587–589. doi: 10.1038/nmeth.4285

Kamruzzaman, M., Beyene, M. A., Siddiqui, A., Ballvora, A., Léon, J., and Naz, A. A. (2022). Pinpointing genomic loci for drought-induced proline and hydrogen peroxide accumulation in bread wheat under field conditions. *BMC Plant Biol.* 22 (1), 584. doi: 10.1186/s12870-022-03943-9

Katoh, K., Rozewicki, J., and Yamada, K. D. (2019). MAFFT online service: Multiple sequence alignment, interactive sequence choice and visualization. *Briefings Bioinf.* 20, 1160–1166. doi: 10.1093/bib/bbx108

Kelley, L. A., Mezulis, S., Yates, C. M., Wass, M. N., and Sternberg, M. J. E. (2015). The Phyre2 web portal for protein modeling, prediction and analysis. *Nat. Protoc.* 10, 845–858. doi: 10.1038/nprot.2015.053

Kendrew, S. G. (2001). YUCCA: A flavin monooxygenase in auxin biosynthesis. *Trends Biochem. Sci.* 26, 218. doi: 10.1016/S0968-0004(01)01814-X

Kolkman, J. A., and Stemmer, W. P. C. (2001). Directed evolution of proteins by exon shuffling. *Nat. Biotechnol.* 19, 423–428. doi: 10.1038/88084

Kong, W., Li, J., Yu, Q., Cang, W., Xu, R., Wang, Y., et al. (2016). Two novel flavin-containing monooxygenases involved in biosynthesis of aliphatic glucosinolates. *Front. Plant Sci.* 7. doi: 10.3389/fpls.2016.01292

Krithika, R., Marathe, U., Saxena, P., Ansari,, Mohd., Z., Mohanty, D., et al. (2006). A genetic locus required for iron acquisition in *Mycobacterium tuberculosis*. *Proc. Natl. Acad. Sci.* 103, 2069–2074. doi: 10.1073/pnas.0507924103

Lenk, M., Wenig, M., Bauer, K., Hug, F., Knappe, C., Lange, B., et al. (2019). Pipecolic acid is induced in barley upon infection and triggers immune responses associated with elevated nitric oxide accumulation. *Mol. Plant-Microbe Interactions®* 32, 1303–1313. doi: 10.1094/MPMI-01-19-0013-R

Lescot, M. (2002). PlantCARE, a database of plant *cis*-acting regulatory elements and a portal to tools for in silico analysis of promoter sequences. *Nucleic Acids Res.* 30, 325–327. doi: 10.1093/nar/30.1.325

Letunic, I., Khedkar, S., and Bork, P. (2021). SMART: Recent updates, new developments and status in 2020. *Nucleic Acids Res.* 49, D458–D460. doi: 10.1093/nar/gkaa937

Letunic, I., and Bork, P. (2021). Interactive Tree Of Life (iTOL) v5: An online tool for phylogenetic tree display and annotation. *Nucl. Acids Res.* 49 (W1), W293–W296. doi: 10.1093/nar/gkab301

Li, H.- Z., Gao, X., Li, X.- Y., Chen, Q.- J., Dong, J., and Zhao, W.- C. (2013). Evaluation of assembly strategies using RNA-Seq data associated with grain development of wheat (*Triticum aestivum L.*). *PLoS ONE* 8 (12), e83530. doi: 10.1371/journal.pone.0083530

Li, J., Hansen, B. G., Ober, J. A., Kliebenstein, D. J., and Halkier, B. A. (2008). Subclade of flavin-monooxygenases involved in aliphatic glucosinolate biosynthesis. *Plant Physiol.* 148, 1721–1733. doi: 10.1104/pp.108.125757

Li, J., Kristiansen, K. A., Hansen, B. G., and Halkier, B. A. (2011). Cellular and subcellular localization of flavin-monooxygenases involved in glucosinolate biosynthesis. *J. Exp. Bot.* 62, 1337–1346. doi: 10.1093/jxb/erq369

Li, N., Yin, N., Niu, Z., Hui, W., Song, J., Huang, C., et al. (2014). Isolation and characterization of three *TaYUC10* genes from wheat. *Gene* 546, 187–194. doi: 10.1016/j.gene.2014.06.020

Li, Q., Zheng, Q., Shen, W., Cram, D., Fowler, D. B., Wei, Y., et al. (2015). Understanding the biochemical basis of temperature-induced lipid pathway adjustments in plants. *Plant Cell* 27 (1), 86–103. doi: 10.1105/tpc.114.134338

Liu, Z., Xin, M., Qin, J., Peng, H., Ni, Z., Yao, Y., et al. (2015). Temporal transcriptome profiling reveals expression partitioning of homologous genes contributing to heat and drought acclimation in wheat (*Triticum aestivum* L.). *BMC Plant Biol.* 15, 152. doi: 10.1186/s12870-015-0511-8

Luo, W., Xiao, N., Wu, F., Mo, B., Kong, W., and Yu, Y. (2022). Genome-wide identification and characterization of *YUCCA* gene family in Mikania micrantha. *Int. J. Mol. Sci.* 23, 13037. doi: 10.3390/ijms232113037

Ma, H., Lin, J., Mei, F., Mao, H., and Li, Q. Q. (2023). Differential alternative polyadenylation of homoeologous genes of allohexaploid wheat ABD subgenomes during drought stress response. *Plant J.* 114, 499–518. doi: 10.1111/tpj.16150

Maddison, W. P., and Maddison, D. R. (2023). Mesquite: a modular system for evolutionary analysis. *Version 3.7*. Available at: http://www.mesquiteproject.org/.

Malito, E., Alfieri, A., Fraaije, M. W., and Mattevi, A. (2004). Crystal structure of a Baeyer–Villiger monooxygenase. *Proc. Natl. Acad. Sci.* 101, 13157–13162. doi: 10.1073/pnas.0404538101

Mangini, G., Blanco, A., Nigro, D., Signorile, M. A., and Simeone, R. (2021). Candidate Genes and quantitative trait loci for grain yield and seed size in durum wheat. *Plants* 10, 312. doi: 10.3390/plants10020312

Mascotti, M. L., Lapadula, W. J., and Juri Ayub, M. (2015). The origin and evolution of Baeyer—Villiger monooxygenases (BVMOs): an ancestral family of flavin monooxygenases. *PloS One* 10, e0132689. doi: 10.1371/journal.pone.0132689

Matros, A., Liu, G., Hartmann, A., Jiang, Y., Zhao, Y., Wang, H., et al. (2017). Genome–metabolite associations revealed low heritability, high genetic complexity, and causal relations for leaf metabolites in winter wheat (Triticum aestivum). *J. Exp. Bot.* 68, erw441. doi: 10.1093/jxb/erw441

Mignone, F., Gissi, C., Liuni, S., and Pesole, G. (2002). Untranslated regions of mRNAs. *Genome Biol.* 3, reviews0004.1. doi: 10.1186/gb-2002-3-3-reviews0004

Mishina, T. E., and Zeier, J. (2006). The Arabidopsis flavin-dependent monooxygenase FMO1 is an essential component of biologically induced systemic acquired resistance. *Plant Physiol.* 141 (4), 1666–1675. doi: 10.1104/pp.106.081257

Mitchell, A. J., and Weng, J.-K. (2019). Unleashing the synthetic power of plant oxygenases: from mechanism to application. *Plant Physiol.* 179, 813–829. doi: 10.1104/pp.18.01223

Navathe, S., Pandey, A. K., Sharma, S., Chand, R., Mishra, V. K., Kumar, D., et al. (2022). New Genomic Regions Identified for Resistance to Spot Blotch and Terminal Heat Stress in an Interspecific Population of *Triticum aestivum* and *T. spelta*. *Plants* 11, 2987. doi: 10.3390/plants11212987

Nussbaumer, T., Warth, B., Sharma, S., Ametz, C., Bueschl, C., Parich, A., et al. (2015). Joint transcriptomic and metabolomic analyses reveal changes in the primary metabolism and imbalances in the subgenome orchestration in the bread wheat molecular response to *Fusarium graminearum*. *G3 Genes|Genomes|Genetics* 5, 2579–2592. doi: 10.1534/g3.115.021550

Per, T. S., Khan, M. I. R., Anjum, N. A., Masood, A., Hussain, S. J., and Khan, N. A. (2018). Jasmonates in plants under abiotic stresses: Crosstalk with other phytohormones matters. *Environ. Exp. Bot.* 145, 104–120. doi: 10.1016/j.envexpbot.2017.11.004

Qi, P.-F., Balcerzak, M., Rocheleau, H., Leung, W., Wei, Y.-M., Zheng, Y.-L., et al. (2016). Jasmonic acid and abscisic acid play important roles in host–pathogen interaction between *Fusarium graminearum* and wheat during the early stages of

fusarium head blight. *Physiol. Mol. Plant Pathol.* 93, 39–48. doi: 10.1016/j.pmpp.2015.12.004

Qin, M., Wang, J., Zhang, T., Hu, X., Liu, R., Gao, T., et al. (2020). Genome-wide identification and analysis on YUCCA gene family in isatis indigotica fort. And iiYUCCA6-1 functional exploration. *Int. J. Mol. Sci.* 21, 2188. doi: 10.3390/ijms21062188

Qiu, Z., Guo, J., Zhu, A., Zhang, L., and Zhang, M. (2014). Exogenous jasmonic acid can enhance tolerance of wheat seedlings to salt stress. *Ecotoxicology Environ. Saf.* 104, 202–208. doi: 10.1016/j.ecoenv.2014.03.014

Ramírez-González, R. H., Borrill, P., Lang, D., Harrington, S. A., Brinton, J., Venturini, L., et al. (2018). The transcriptional landscape of polyploid wheat. *Science* 361, eaar6089. doi: 10.1126/science.aar6089

R Core Team. (2021). *R: A language and environment for statistical computing* (Vienna, Austria: R Foundation for Statistical Computing). Available at: https://www.R-project.org/.

Roosens, N. H. C. J., Thu, T. T., Iskandar, H. M., and Jacobs, M. (1998). Isolation of the Ornithine-δ-Aminotransferase cDNA and Effect of Salt Stress on Its Expression in Arabidopsis thaliana 1. *Plant Physiol.* 117, 263–271. doi: 10.1104/pp.117.1.263

Rossner, R., Kaeberlein, M., and Leiser, S. F. (2017). Flavin-containing monooxygenases in aging and disease: Emerging roles for ancient enzymes. *J. Biol. Chem.* 292, 11138–11146. doi: 10.1074/jbc.R117.779678

Rudd, J. J., Kanyuka, K., Hassani-Pak, K., Derbyshire, M., Andongabo, A., Devonshire, J., et al. (2015). Transcriptome and metabolite profiling of the infection cycle of *Zymoseptoria tritici* on wheat reveals a biphasic interaction with plant immunity involving differential pathogen chromosomal contributions and a variation on the hemibiotrophic lifestyle definition. *Plant Physiol.* 167, 1158–1185. doi: 10.1104/pp.114.255927

Sahu, R., Prabhakaran, N., Kundu, P., and Kumar, A. (2021). Differential response of phytohormone signaling network determines nonhost resistance in rice during wheat stem rust (*Puccinia graminis* f. Sp. *Tritici*) colonization. *Plant Pathol.* 70, 1409–1420. doi: 10.1111/ppa.13376

Schall, P., Marutschke, L., and Grimm, B. (2020). The flavoproteome of the model plant *Arabidopsis thaliana*. *Int. J. Mol. Sci.* 21, 5371. doi: 10.3390/ijms21155371

Schlaich, N. L. (2007). Flavin-containing monooxygenases in plants: Looking beyond detox. *Trends Plant Sci.* 12, 412–418. doi: 10.1016/j.tplants.2007.08.009

Schnake, A., Hartmann, M., Schreiber, S., Malik, J., Brahmann, L., Yildiz, I., et al. (2020). Inducible biosynthesis and immune function of the systemic acquired resistance inducer *N*-hydroxypipecolic acid in monocotyledonous and dicotyledonous plants. *J. Exp. Bot.* 71, 6444–6459. doi: 10.1093/jxb/eraa317

Schrödinger, L., and DeLano, W. (2020). PyMOL. Available at: http://www.pymol.org/pymol.

Schweiger, W., Steiner, B., Vautrin, S., Nussbaumer, T., Siegwart, G., Zamini, M., et al. (2016). Suppressed recombination and unique candidate genes in the divergent haplotype encoding Fhb1, a major *Fusarium* head blight resistance locus in wheat. *Theor. Appl. Genet.* 129, 1607–1623. doi: 10.1007/s00122-016-2727-x

Shumayla and Upadhyay, S. K. (2023). "An overview of receptor-like kinases in plants," in *Plant Receptor-Like Kinases* (Elsevier), 1–23. doi: 10.1016/B978-0-323-90594-7.00005-3

Song, C., Zhang, D., Zheng, L., Shen, Y., Zuo, X., Mao, J., et al. (2020). Genome-wide identification and expression profiling of the *YUCCA* gene family in Malus domestica. *Sci. Rep.* 10, 10866. doi: 10.1038/s41598-020-66483-y

Srivastava, A. K., Lu, Y., Zinta, G., Lang, Z., and Zhu, J.-K. (2018). UTR-dependent control of gene expression in plants. *Trends Plant Sci.* 23, 248–259. doi: 10.1016/j.tplants.2017.11.003

Stehr, M., Diekmann, H., Smau, L., Seth, O., Ghisla, S., Singh, M., et al. (1998). A hydrophobic sequence motif common to *N*-hydroxylating enzymes. *Trends Biochem. Sci.* 23, 56–57. doi: 10.1016/S0968-0004(97)01166-3

Teufel, F., Almagro Armenteros, J. J., Johansen, A. R., Gíslason, M. H., Pihl, S. I., Tsirigos, K. D., et al. (2022). SignalP 6.0 predicts all five types of signal peptides using protein language models. *Nat. Biotechnol.* 40, 1023–1025. doi: 10.1038/s41587-021-01156-3

The International Wheat Genome Sequencing Consortium (IWGSC), Appels, R., Eversole, K., Stein, N., Feuillet, C., Keller, B., et al. (2018a). Shifting the limits in wheat research and breeding using a fully annotated reference genome. *Science* 361, eaar7191. doi: 10.1126/science.aar7191

Thodberg, S., and Jakobsen Neilson, E. H. (2020). The "Green" FMOs: diversity, functionality and application of plant flavoproteins. *Catalysts* 10, 329. doi: 10.3390/catal10030329

Thodberg, S., Sørensen, M., Bellucci, M., Crocoll, C., Bendtsen, A. K., Nelson, D. R., et al. (2020). A flavin-dependent monooxygenase catalyzes the initial step in cyanogenic glycoside synthesis in ferns. *Commun. Biol.* 3, 507. doi: 10.1038/s42003-020-01224-5

Tichtinsky, G., Vanoosthuyse, V., Cock, J. M., and Gaude, T. (2003). Making inroads into plant receptor kinase signaling pathways. *Trends Plant Sci.* 8, 231–237. doi: 10.1016/S1360-1385(03)00062-1

Vicient, C. M., and Casacuberta, J. M. (2017). Impact of transposable elements on polyploid plant genomes. *Ann. Bot.* 120, 195–207. doi: 10.1093/aob/mcx078

Vikas, V. K., Pradhan, A. K., Budhlakoti, N., Mishra, D. C., Chandra, T., Bhardwaj, S. C., et al. (2022). Multi-locus genome-wide association studies (ML-GWAS) reveal novel genomic regions associated with seedling and adult plant stage leaf rust resistance in bread wheat (*Triticum aestivum* L.). *Heredity* 128, 434–449. doi: 10.1038/s41437-022-00525-1

Visca, P., Ciervo, A., and Orsi, N. (1994). Cloning and nucleotide sequence of the pvdA gene encoding the pyoverdin biosynthetic enzyme L-ornithine N5-oxygenase in *Pseudomonas aeruginosa*. *J. Bacteriology* 176, 1128–1140. doi: 10.1128/jb.176.4.1128-1140.1994

Vlot, A. C., Sales, J. H., Lenk, M., Bauer, K., Brambilla, A., Sommer, A., et al. (2021). Systemic propagation of immunity in plants. *New Phytol.* 229 (3), 1234–1250. doi: 10.1111/nph.16953

Wang, Y., Tang, H., DeBarry, J. D., Tan, X., Li, J., Wang, X., et al. (2012). MCScanX: A toolkit for detection and evolutionary analysis of gene synteny and collinearity. *Nucleic Acids Res.* 40, e49–e49. doi: 10.1093/nar/gkr1293

Wong, T. K., Kalyaanamoorthy, S., Meusemann, K., Yeates, D., Misof, B., and Jermiin, L. (2014). *AliStat version 1.3* (CSIRO). Canberra, Australia. doi: 10.4225/08/59309DA8368E1

Xue, X., Liu, A., and Hua, X. (2009). Proline accumulation and transcriptional regulation of proline biosynthesis and degradation in *Brassica napus*. *BMB Rep.* 42, 28–34. doi: 10.5483/BMBRep.2009.42.1.028

Yamamoto, Y., Kamiya, N., Morinaka, Y., Matsuoka, M., and Sazuka, T. (2007). Auxin biosynthesis by the *YUCCA* genes in rice. *Plant Physiol.* 143, 1362–1371. doi: 10.1104/pp.106.091561

Yang, F., Li, W., and Jørgensen, H. J. L. (2013). Transcriptional Reprogramming of Wheat and the Hemibiotrophic Pathogen *Septoria tritici* during Two Phases of the Compatible Interaction. *PloS One* 8, e81606. doi: 10.1371/journal.pone.0081606

Yang, Y., Xu, T., Wang, H., and Feng, D. (2021). Genome-wide identification and expression analysis of the *TaYUCCA* gene family in wheat. *Mol. Biol. Rep.* 48, 1269–1279. doi: 10.1007/s11033-021-06197-0

Yang, Z., Peng, Z., Wei, S., Liao, M., Yu, Y., and Jang, Z. (2015). Pistillody mutant reveals key insights into stamen and pistil development in wheat (*Triticum aestivum L.*). *BMC Genomics* 16 (1), 211. doi: 10.1186/s12864-015-1453-0

Yoshimoto, N., Onuma, M., Mizuno, S., Sugino, Y., Nakabayashi, R., Imai, S., et al. (2015). Identification of a flavin-containing *S* -oxygenating monooxygenase involved in alliin biosynthesis in garlic. *Plant J.* 83, 941–951. doi: 10.1111/tpj.12954

Yoshimoto, N., and Saito, K. (2015). "Identification of genes potentially encoding S-oxygenation enzymes for the biosynthesis of S-alk(en)yl-l-cysteine sulfoxides in onion," in *Molecular Physiology and Ecophysiology of Sulfur*. Eds. L. J. De Kok, M. J. Hawkesford, H. Rennenberg, K. Saito and E. Schnug (Cham: Springer International Publishing), 201–204. doi: 10.1007/978-3-319-20137-5_21

Yu, Y., Ouyang, Y., and Yao, W. (2018). shinyCircos: An R/Shiny application for interactive creation of Circos plot. *Bioinformatics* 34, 1229–1231. doi: 10.1093/bioinformatics/btx763

Yu, J., Xuan, W., Tian, Y., Fan, L., Sun, J., Tang, W., et al. (2021). Enhanced OsNLP4-OsNiR cascade confers nitrogen use efficiency by promoting tiller number in rice. *Plant Biotechnol. J.* 19, 167–176. doi: 10.1111/pbi.13450

Zhang, C., Huang, L., Zhang, H., Hao, Q., Lyu, B., Wang, M., et al. (2019). An ancestral NB-LRR with duplicated 3′UTRs confers stripe rust resistance in wheat and barley. *Nat. Commun.* 10, 4023. doi: 10.1038/s41467-019-11872-9

Zhang, K., Zhang, J., Cui, C., Chai, L., Zheng, B., Jiang, J., et al. (2022). Genome-wide identification and expression profiling of the *YUCCA* gene family in *Brassica napus*. *Oil Crop Sci.* 7, 103–111. doi: 10.1016/j.ocsci.2022.07.001

Zhang, E. T., Zhang, H., and Tang, W. (2021). Transcriptomic analysis of wheat seedling responses to the systemic acquired resistance inducer *N*-hydroxypipecolic acid. *Front. Microbiol.* 12. doi: 10.3389/fmicb.2021.621336

Zhao, Y. (2014). Auxin biosynthesis. *The Arabidopsis Book*. 12, e0173. doi: 10.1199/tab.0173

Zhao, Y., Christensen, S. K., Fankhauser, C., Cashman, J. R., Cohen, J. D., Weigel, D., et al. (2001). A role for flavin monooxygenase-like enzymes in Auxin biosynthesis. *Science* 291, 306–309. doi: 10.1126/science.291.5502.306

Zhao, P., Ma, X., Zhang, R., Cheng, M., Niu, Y., Shi, X., et al. (2023). Integration of genome-wide association study, linkage analysis, and population transcriptome analysis to reveal the *TaFMO1-5B* modulating seminal root growth in bread wheat. *Plant J.* 116, 1385–1400. doi: 10.1111/tpj.16432

Zhou, C., Dong, Z., Zhang, T., Wu, J., Yu, S., Zeng, Q., et al. (2020). Genome-Scale Analysis of Homologous Genes among Subgenomes of Bread Wheat (*Triticum aestivum* L.). *Int. J. Mol. Sci.* 21, 3015. doi: 10.3390/ijms21083015

Zhu, Y., Li, H., Su, Q., Wen, J., Wang, Y., Song, W., et al. (2019). A phenotype-directed chemical screen identifies ponalrestat as an inhibitor of the plant flavin monooxygenase YUCCA in auxin biosynthesis. *J. Biol. Chem.* 294, 19923–19933. doi: 10.1074/jbc.RA119.010480

Zhu, T., Wang, L., Rimbert, H., Rodriguez, J. C., Deal, K. R., De Oliveira, R., et al. (2021). Optical maps refine the bread wheat *Triticum aestivum* cv. Chinese Spring genome assembly. *Plant J.* 107, 303–314. doi: 10.1111/tpj.15289

Glossary

FMO	Flavin-containing monooxygenase
'nc'	non-canonical
FAD	flavin adenine dinucleotide
NAD(P)H	nicotinamide adenine dinucleotide phosphate
MSA	multiple sequence alignment
FPKM	Fragments Per Kilobase of transcript per Million mapped reads
Tpm	transcripts per million